RSC Advances

PAPER

View Article Online
View Journal | View Issue

Cite this: *RSC Adv.*, 2026, **16**, 24325

Waste-to-worth: nano activated carbon from fruit peels for sulfur-free sugarcane juice clarification

Ramesh Duraisamy,[a] Wabi Regasa Bogale[ab] and Gada Muleta Fanta *[acd]

The sugar industry faces significant challenges in achieving high purity and maximizing yield during production, particularly in the crucial clarification stage. Effective clarifying agents are essential for this process. Activated carbon has emerged as a highly suitable adsorbent for removing impurities from sugarcane juice, due to its strong adsorption capacity. This study focuses on preparing nano activated carbon (NAC) derived from mixed fruit peels for clarifying sugarcane juice. Using Design-Expert software, we optimized the experimental parameters for NAC production, determining the optimal conditions: carbonization at 410 °C for 100 min with an acid impregnation ratio of 1. Under these conditions, the resulting NAC achieved a yield of 74.86%, a fixed carbon content of 89.25 ± 0.38%, and a specific surface area of 650.87 ± 0.26 m^2 g^{-1}. Characterization by X-ray diffraction and scanning electron microscopy revealed that the NAC had an average particle size of 24.46 nm, with a predominant particle size distribution between 20 and 30 nm. The optimization of NAC for cane juice clarification yielded impressive results under optimal conditions: a NAC dose of 0.01%, pH of 4, temperature of 90 °C, duration of 20 min, and agitation speed of 100 rpm, resulting in a turbidity reduction to 1760.6 NTU, a settling rate of 0.09 cm min^{-1}, a mud volume of 6.66 mL per 100 mL, and a color removal efficiency of 97.4%. Additionally, we examined the physicochemical properties of the NAC, the juice posttreatment, and the final sugar product. The findings demonstrate that NAC synthesized from mixed fruit peels exhibits a high carbon yield and a high specific surface area, highlighting its potential as an effective biosorption material. The synthesized NAC demonstrated excellent clarification efficiency, making it an advantageous clarifying agent for sugarcane juice processing and sulfur-free sugar production. This research has significant implications for waste management, particularly in reducing landfill pollution, while also contributing to the development of value-added products that enhance bioresource management.

Received 17th February 2026
Accepted 26th April 2026

DOI: 10.1039/d6ra01408a

rsc.li/rsc-advances

1 Introduction

Sugarcane (*Saccharum officinarum*) and sugar beets (*Beta vulgaris*) are the primary sources for producing table sugar (sucrose). The industrial process for extracting sucrose involves several steps of isolation and purification to separate it from non-sugar components. Traditional cane sugar production involves four main activities: purifying the raw juice extracted from the cane, evaporating the clarified juice, crystallizing the syrup, and separating the sucrose crystals from molasses (the thick liquid containing uncrystallized sucrose).[1] To remove color and colloidal substances from sugarcane juice, it undergoes clarification through coagulation, flocculation, and precipitation. This process may result in an insoluble precipitate that effectively absorbs and extracts undesired components from the juice, followed by decanting and filtration.[2] The liming process produces a low-turbidity liquor but may result in higher mud levels and slower-settling flocs. Additionally, the clarified juice may contain higher levels of calcium, which can cause scaling in evaporators.[3]

Alternative methods for clarifying cane juice include the use of synthetic polymer acrylamide, which accelerates the settling of impurities. However, this method is expensive and has raised concerns regarding potential cancer and neurotoxicity risks.[4] Furthermore, many countries are moving away from using SO_2 in the sulfitation process for refining sugar due to the health risks associated with residual sulfur in sugar products,[4] and it is an expensive treatment, requiring the use of SO_2 in addition to the health issues. There is growing interest in developing cost effective, efficient alternatives to conventional commercial clarifying agents. Exploring the use of affordable, effective activated carbon (AC) not only promotes environmental

[a]*Department of Chemistry, College of Natural and Computational Sciences, Arba Minch University, P.O. Box 21, Arba Minch, Ethiopia*
[b]*Department of Industrial Chemistry, College of Natural and Computational Sciences, Bule Hora University, P.O. Box 144, Bule Hora, Ethiopia*
[c]*Department of Materials Science and Engineering, Adama Science and Technology University, P.O. Box 1888, Adama, Ethiopia. E-mail: gada.muleta@astu.edu.et*
[d]*Center of Advanced Materials Science and Engineering, Adama Science and Technology University, P.O. Box 1888, Adama, Ethiopia*

sustainability but also offers benefits for future commercial applications.[5]

Nano activated carbon is gaining immense popularity for its ability to purify and remove pollutants from water, due to its significantly larger surface area and higher adsorption rates than traditional bulk AC. This cutting-edge technology offers a faster, more efficient alternative to conventional water purification methods, resulting in higher impurity removal in aqueous media.[6,7] Among the various options, nano activated carbon (as adsorbents) stands out as a cost-effective solution for treating contaminated water due to its unique characteristics, availability, and high efficacy with smaller particles (on the nanometer scale, 10^{-9} meters), in contrast to regular activated carbon (AC), which has larger particles measured in micrometers.[8,9]

Agro by-products have emerged as promising raw materials for producing activated carbon (AC). Recent advances in using fruit peels as precursors for AC underscore growing interest in converting agricultural waste into value-added products. According to Lee *et al.*,[10] fruit peels, often abundant and discarded, are a potential source of carbonized materials because of their high content of cellulose, hemicellulose, and lignin, key components of carbonized materials. Studies have investigated the viability of using fruit peels from citrus fruits (such as oranges, lemons, and grapefruits), bananas, mangoes, and pineapples as precursors for AC synthesis.[9,11–16]

The preparation of nano activated carbon from fruit peel waste represents a groundbreaking interdisciplinary research initiative that merges materials science, waste management, and nanotechnology to create sustainable, high-performance carbonaceous materials with a wide range of applications. This activated carbon can be used as an adsorbent or clarifier to effectively remove pollutants from wastewater and industrial effluents.[9,13–15] Additionally, it can be expected to remove impurities (non-sucrose materials) from sugarcane juice during the sugar manufacturing process.

Research in this field has concentrated on fine-tuning activation conditions to enhance the porosity, surface area, and adsorption characteristics of the resulting activated carbon (AC) materials.[17] Various factors, including temperature, duration, and impregnation ratio during carbon material activation, have been investigated to optimize the yield and quality of AC produced from fruit peels. The use of phosphoric acid (H_3PO_4) as an activating agent in the synthesis of activated carbon involves a chemical activation process that transforms carbonaceous precursors into porous structures, yielding greater surface areas and adsorption capacities than with other activating agents.[7–9]

The costs associated with chemically treating sugarcane juice and the environmental pollution resulting from sludge disposal have prompted the exploration of innovative materials such as NAC.[3,9] Research has shown that certain cellulosic materials in fruit peel waste and sugarcane bagasse can be converted into nano activated carbon. Similarly, alternative clarifiers using the cane juice clarification approach substitute traditional chemical treatments with NAC-like materials derived from fruit peel waste, such as banana, avocado, and papaya peels. Utilizing mixed fruit peel waste with a higher organic carbon content to produce activated carbon represents an alternative method for recycling resources and generating value-added products that enhance its adsorption capacity, selectivity, and stability.[18,19]

Activated carbon made from fruit peel (a form of agricultural carbon, in nano-scale, NAC) has shown promising cost-effective cane juice clarifier, with studies on similar biomass carbons (like bagasse AC) reporting up to 98% color removal under lab conditions without chemical additives, which is comparable to the performance of commercial powdered activated carbon.[20] In contrast, conventional clarification methods such as SO_2 (sulfitation) and carbonation (lime + CO_2) remain industry standards but can introduce residual chemicals (*e.g.*, sulfur) and require precise pH/temperature control.

Commercial PAC or GAC combined with lime generally improves turbidity and color, but at a higher cost and sometimes greater sludge generation than biomass NAC. Polymers like those in polysaccharides enhance flocculation, but synthetic residues and dosing complexity also affect flocculation.[21,22] A control sample with no clarifier typically yields poor color and high turbidity, highlighting that NAC from fruit peels not only achieves effective impurity adsorption analogous to commercial PAC/GAC under identical conditions but also offers a practical advantage of reduced chemical usage, lower cost, and minimal residual contaminants in the clarified juice.[20]

The novelty of this study, which focused on preparing NAC from mixed fruit peels (from avocado, banana, and papaya), lies in mixing heterogeneous agro-wastes into a single nanoscale carbon precursor, producing synergistically improved pore structures and surface functionalities compared with single-biomass sources. In contrast, the mixed-peel approach achieved compositional diversity (cellulose, lignin, pectin, polyphenols) to produce hierarchical nano-porosity and improved biomass strategy; therefore, it represents a more sustainable and possibly higher-performance pathway for nano-carbon production compared with conventional single-precursor methods. This novelty contributes to improved sustainability, waste reduction, and multifunctional performance compared with traditional single-biomass activated carbons. Continued research in this area is expected to optimize the production process further and expand the use of cellulose derived from fruit peels across various technological and environmental applications in terms of mixed fruit peel-derived NAC, which reduces organic waste accumulation and provides a low-cost, eco-friendly adsorbent for minimizing pollutants/organic materials (from aqueous media) and reliance on non-renewable materials.

The possibility of using NAC derived from mixed fruit peel (MFP) to clarify cane juice has not been examined in the existing literature, offering an opportunity to safeguard the environment from pollution while benefiting local communities and the industrial sector. Hence, the main objective of this research focuses on the preparation, optimization, and characterization of an effective NAC derived from fruit peel waste for clarifying sugarcane juice. Specifically, we developed cost-effective NACs using a mixture of banana, papaya, and avocado peels (as MFP).

This study also investigated the effects of temperature, time, and acid impregnation ratio on the mixed fruit peel powder during the preparation of nano activated carbon (NAC). Additionally, it assessed the morphological, structural, and particle size characteristics of the NACs. Furthermore, the research explored a novel source of nano activated carbon for clarifying sugarcane juice, with potential applications in the sugar industry.

2. Materials and methods

2.1. Sample collection

In this study, waste from mixed fruit peels, specifically avocado, banana, and papaya, was utilized as a precursor. In February 2024, samples of each peel type were collected separately using a random sampling method in Arbaminch, southern Ethiopia, East Africa. The samples were placed in separate moisture-free polyethene bags and promptly transported to the laboratory for further processing.

2.2. Selection and preparation of mixed fruit peel powder

In this study, the peels were selected based on local abundance and their complementary proximate composition, as these peels are widely generated agro-wastes and differ in carbon yield and ash content. The report indicates that banana peel contains high volatile matter, and papaya peel contributes lower ash and higher oxygenated groups. In contrast, avocado peel yields higher lignin and carbon, which are favorable for NAC preparation.[23,24] Therefore, blending reflects a material-driven rationale rather than random selection.

The collected fruit peels were thoroughly cleaned in the laboratory using tap water to remove any dirt or debris. After cleaning, they were sliced and dried in an oven at 110 °C for 24 h until sufficiently dry for grinding into powder. The dried peels were then ground in a laboratory grinder.[25] and passed through a 500 micrometre sieve to ensure uniform particle size. The ground peel powders were blended to a total of 100 g at various proportions, as outlined in Table S1. The resulting finely powdered, homogenized fruit peel samples were stored in a moisture-proof, airtight container until they were activated and carbonized.[26] Additional details on the optimization of the mixing proportions for the fruit peels are available in the SI.

2.3. Preparation and optimization of nano activated carbon

The process consisted of a single step that involved activation and carbonization to optimize the proportions of the fruit peel. This was achieved by activating the optimized proportions of dried mixed fruit peel, then carbonizing them in a fruit peel mixer. The experimental design used the RSM-CCD quadratic model approach, as detailed in Table S1. The independent variables included factor *A*, which represented the impregnation ratio (between sample and acid) of the fruit peel with phosphoric acid (40% H_3PO_4) at varying levels (1 to 2); factor *B*, which indicated the processing temperature range (400–700 °C); and factor *C*, which pertained to the processing time (40–100 min). These processing conditions were selected based on previous research.[27–29]

Optimized dried, powdered mixed peel waste samples (100 g) were treated with 40% H_3PO_4 at varying ratios, as detailed in Table S1. The treated mixture was then placed in an oven at 100 °C for 12 h to eliminate moisture. Following this, the dried samples were activated at different temperatures and activation

Table 1 Experimental designs of fruit peel powder mixing proportions and the response (carbon yield) for the optimization under RSM[a]

	Independent variables: amount of fruit peels (g)			Dependent variable: % carbon yield	
Run	A: Avocado peel (g)	B: Banana peel (g)	C: Papaya peel (g)	Experiment results	Predicted results
1	27.03	27.03	45.94	70.36 ± 0.32 ^{cd}	70.42
2	14.3	42.85	42.85	69.11 ± 0.24^{d}	69.05
3	42.85	42.85	14.3	73.84 ± 0.21^{a}	73.80
4	33.33	33.33	33.34	71.77 ± 0.67^{b}	71.72
5	42.85	14.3	42.85	71.23 ± 0.30^{bc}	71.18
6	43.5	43.5	13.0	71.31 ± 0.32^{bc}	71.35
7	27.03	45.94	27.03	69.80 ± 0.37^{d}	69.85
8	45.94	27.03	27.03	73.32 ± 0.49^{a}	73.37
9	43.5	13.0	43.5	74.92 ± 0.34^{a}	73.97
10	33.33	33.33	33.34	67.52 ± 0.61^{e}	67.47
11	33.33	33.33	33.34	71.77 ± 0.67^{b}	71.72
12	13.0	43.5	43.5	66.05 ± 0.62^{f}	66.10
ANOVA model summary: Reg. coefficient, R^2				0.9996	
Adjusted R^2				0.9976	
Predicted R^2				0.9469	
Adeq precision				72.6031	
p-value				0.0019	
CV				0.1676	

[a] Data expressed as means ± standard deviation of triplicate experiments ($n = 3$); mean values (in the column) share different superscripts, which are called significantly different ($p < 0.05$).

durations, as specified in Table 1, ranging from 40 to 100 min.[27,29] After activation, the activated carbon (AC) was cooled to room temperature and rinsed with distilled water until the wash water was neutral. Finally, the AC was dried in an oven at 105 °C overnight.

After drying, the synthesized activated carbon was ground, sieved, and stored in a glass bottle until ready for analysis.[29] All prepared activated carbons were assessed and optimized for their high fixed carbon content and surface area using Design-Expert software (v.13.0.5.0, USA) to evaluate the adsorbent material.

2.4. Characterization of MFP and NAC

This study aims to enhance the quality of raw materials and prepared products by examining the physicochemical properties of mixed fruit peels (MFP) and the activated carbon produced from them. Key characteristics assessed include moisture, ash content, volatile matter, fixed carbon, carbon yield, and active surface area.[26,30] Additionally, Fourier transform infrared spectroscopy (FTIR) was used to analyze changes in functional groups in the optimized NAC. The surface morphology of the NAC was investigated using scanning electron microscopy (SEM), and X-ray diffraction (XRD) was used to evaluate the crystalline structure and particle size of the synthesized and optimized NAC.

2.4.1. Physicochemical characterizations of MFP and NAC.

The physicochemical properties of the samples were assessed by heating them to a designated temperature. The analysis of moisture, volatile matter, ash, and fixed carbon content was conducted in accordance with previously established literature.[31,32]

2.4.1.1. Moisture content. To estimate the moisture content of MFP and NAC, 10 g of each sample was weighed and transferred into a pre-weighed Petri dish. The dish containing the sample was then placed in a hot air oven at 105 ± 0.5 °C for 3 hours to ensure complete drying. The percentage moisture was calculated using the following eqn (1):

$$\text{The moisture content of MFPW (\%)} = [(C - D)/(C - B)] \times 100 \quad (1)$$

B represents the weight of the Petri dish, C indicates the weight of the Petri dish combined with the original sample, and D reflects the weight of the Petri dish along with the dried sample.

2.4.1.2. Volatile matter. The sample (10 g) was weighed and transferred to a pre-weighed crucible, which was then covered with its lid. The crucible was heated in a muffle furnace at 950 °C for 7 min. After cooling, the crucible was reweighed to assess the residual mass. The weight loss of the sample was calculated as follows:

$$\text{Weight loss (\%)} = [(C - D)/(C - B)] \times 100 \quad (2)$$

B represents the mass of the crucible and lid (in g), C denotes the mass of the crucible with the lid and sample (in g), and D indicates the mass of the crucible with the lid and the non-volatile residue (in g). The volatile matter can be calculated using the following formula:

$$\text{Volatile matter content, VM (\%)} = \text{Weight loss (\%)} - \text{Moisture content (\%)} \quad (3)$$

2.4.1.3. Ash content. To assess the ash content, we first weighed 10 g of the dried sample and placed it into a pre-weighed crucible. The sample was then incinerated in a muffle furnace at 650 °C for 3 h. After allowing the crucible to cool, we reweighed it to determine the mass of the residual ash. The ash content of the sample was calculated using eqn (4):

$$\text{Ash content (\%)} = [(C - D)/(C - B)] \times 100 \quad (4)$$

where B represents the weight of the crucible, C denotes the weight of the crucible plus the original sample, and D indicates the weight of the crucible plus the ashed sample.

2.4.1.4. Fixed carbon content. Fixed carbon refers to the solid combustible residue remaining after the removal of volatile matter, moisture, and ash from a sample. It is calculated by subtracting the total of volatile matter, moisture, and ash content from 100.

$$\text{Percent fixed carbon} = 100 - (\text{volatile matter} + \text{ash} + \text{moisture}) \quad (5)$$

2.4.1.5. Percentage of carbon yield of NAC. The weight of the mixed fruit peel and the NAC produced was measured using an electronic balance. The carbon yield for each sample was calculated using the following equation:[33]

$$\text{Carbon yield (\%)} = (\text{Weight of NAC produced/Weight of mixed fruit peel}) \times 100 \quad (6)$$

2.4.1.6. Measurement of the active surface area using the iodine adsorption method. Activated carbon is well known for its extensive surface area, attributed to its porous structure that creates numerous adsorption sites. As the surface area expands, its ability to adsorb molecules, such as iodine, also increases. This correlation arises from the greater availability of adsorption sites on the carbon surface. Consequently, higher iodine values are associated with activated carbons that possess larger surface areas. This relationship is frequently leveraged across several industries that use activated carbon for purification, filtration, and adsorption.[34]

As outlined in the literature,[26,34] the adsorption of I_2 from solution is a common method for evaluating the surface area of activated carbon. The surface area of the prepared NAC was determined using the iodine adsorption method described by Al Jebur & Alwan,[26] with some minor modifications. This technique quantifies the surface area of NAC by measuring the amount of iodine ions adsorbed per gram of NAC. To assess the surface area, 1 g of the prepared NAC was combined with 2 mL of 5% HCl and heated at room temperature for 30 min. Following this, the mixture was added to 100 mL of a 0.1 N iodine solution (N_1) and shaken for an additional 30 min. The resulting solution was then filtered, and 10 mL of the filtrate

was transferred to a conical flask. The iodine content in 10 mL of the filtrate was titrated with 0.1 N anhydrous sodium thiosulfate (N_2) in the presence of a starch indicator. The volume of anhydrous sodium thiosulfate used during the titration was recorded to calculate the iodine number of the NAC, which reflects the amount of iodine adsorbed. The same procedure was used for the blank (without the NAC). Then, the iodine of NAC adsorption was utilized to calculate the surface area of the NAC using the following equation:[26]

$$\text{Adsorbed weight of iodine } (W_I, \text{ in mg } I_2) = a - [2.2 \times b \times (v)].$$

Here, $a = N_1 \times 126.93$; $b = N_2 \times 126.93$; v is the volume of anhydrous sodium thiosulfate.

$$\text{Iodine number (mg } I_2\text{/g of NAC)} = (1.6\ W_I/\text{Weight of NAC} \times \text{Correction coefficient}) \quad (7)$$

Here, N_1 is the concentration of iodine solution; N_2 is the concentration of sodium thiosulfate. 126.93 is the equivalent weight of iodine. According to Wiji's method of I_2 estimation, the correction coefficient (which has a value close to 1.0), which is proposed as a common approximation used to convert the iodine number to surface area as: Surface area ($m^2\ g^{-1}$) $\approx$ iodine number (mg g^{-1}) $\times$ 1.0. It typically uses a correlation of 1 mg $I_2 \approx 1\ m^2$ of surface area supported by ASTM D4607.

2.4.1.7. Point of zero charge. The point of zero charge (PZC) of a material is defined as the pH at which the positive and negative charges on its surface balance each other, resulting in a net charge of zero. To determine the PZC of NAC, the pH drift method was employed. In this procedure, 0.03 g of NAC is added to 50 mL of 0.1 M KNO_3 solution in an Erlenmeyer flask. The pH of the solution is then adjusted to various values ranging from 1 to 12 using HCl or NaOH. After sealing the flask, it is allowed to sit at room temperature for 48 h. The pH of the solution is subsequently measured again. The PZC is identified as the pH at which the initial and final pH values are identical.[35]

2.4.2. X-ray diffraction study. The crystalline and amorphous properties, as well as the orientation within the matrix material (NACs), were evaluated through X-ray diffraction (XRD) analysis conducted by Shimzan Corporation, Japan. This technique analyzed variations in the scattered intensity of an X-ray beam as a function of incident and scattered angles, polarization, and wavelength or energy as it interacted with the material's surface.[30]

2.4.3. Fourier transform infrared spectroscopic study. Fourier transform infrared (FTIR) spectroscopy is a method utilized to identify both organic and inorganic components in a sample. In this study, FTIR (PerkinElmer, Spectrum 650, Germany) was employed to analyze the functional groups present in the prepared MFP and NAC samples. The infrared spectra were recorded over a range of 4000 cm^{-1} to 400 cm^{-1}. The collected data were documented, and the corresponding spectrum was generated using specialized FTIR software.[30]

2.4.4. Scanning electron microscopy study for NAC. The NAC sample was secured to the sample stub with double-sided sticky tape. The specimen holder was then affixed to the stub and transferred to the vacuum chamber, where the SEM (JSM-6390, Eindhoven, Netherlands) scanned the sample with an electron beam. The SEM images were captured using the equipment's built-in software, with photographs taken at various magnifications.[36]

2.5. Extraction of cane juice

Cane juice was extracted from the selected sugarcane using the method outlined.[37] The cane was thoroughly washed with tap water and cleaned before milling. A pre-measured amount of cane was sliced and processed in a laboratory mill to extract the juice. The juice was collected in a clean, moisture-free plastic container. A portion of the extracted juice was stored in the refrigerator for subsequent analysis and processing. The juice yield was calculated using eqn (8):

$$\text{Juice\%} = \frac{\text{wt of sample} - \text{wt of bagasse}}{\text{wt of sample}} \times 100 \quad (8)$$

2.6. Experimental design for optimization of cane juice clarification using NAC

The ideal processing conditions for clarifying extracted cane juice (maintaining a constant juice volume of 100 mL) were determined using a central composite design (CCD) within a response surface methodology framework, facilitated by Design-Expert software (v. 13.0.5.0, USA). Details of the experimental design and the associated procedures for optimizing the clarification of cane juice with NAC are provided in Table S2.

2.7. Production of raw sugar

Clarified juice was evaporated to remove water while maintaining a temperature of 102 °C in a temperature-controlled water bath. This process removed most of the water, forming syrup (concentrated juice). The syrup was then allowed to crystallize at room temperature. To initiate crystallization, a small amount of seed sucrose crystals was added, which initiated the formation of sugar (sucrose). To minimize residual water, a freeze dryer was used. Subsequently, the sugar crystals were separated from the molasses by centrifugation. The sugar was then dried in a conventional oven at 105 °C for 15 minutes. Once dried and cooled, the sugar was stored in a moisture-free container until further analysis. The percentage yield of the produced sugar was calculated by comparing the mass of the sugar obtained to the mass of the clarified juice.

2.8. Physicochemical characterization of raw cane juice, clarified cane juice, and produced raw sugar

Physicochemical analyses were conducted on raw cane juice, clarified cane juice, and raw sugar. The findings for raw cane juice were compared with those for clarified cane juice, and the results for raw sugar were evaluated against international sugar quality standards.

2.8.1. Measuring the settling rate of juice. Clarified juice (100 mL) was placed in a measuring cylinder to monitor

sedimentation height over time until the settling rate reached 1 cm per 20 min, measured at intervals over a total of 100 min.[22] Subsequently, the juice was combined with a specific dose of adsorbent in a beaker. After mixing, the juice was poured into settling tubes, and the level of the sediment interface was recorded at 20, 40, 60, 80, and 100 min, or until no further changes in level were observed. The experiment concluded with the settling rate (in cm min^{-1}), representing the distance travelled over time.

2.8.2. Measuring the mud volume. The clarified juice was poured into 100 mL measuring cylinders and left undisturbed for 20 min. to settle. After allowing for a total sedimentation time of 100 min, we visually assessed the final sediment level. We recorded the sediment height after establishing three boundary lines: the interface between the solid and liquid phases, the clarified juice, and the mud, as demonstrated in a previous study.[38]

2.8.3. Turbidity. The turbidimeter was utilized to assess the turbidity of the samples, which consisted of 100 mL of both raw and clarified juice.[39] The turbidity of each sample was measured and documented in NTU.

2.8.4. Color measurement. The color of both the raw and clear juices was evaluated according to the method outlined by the South African Sugar Technologists' Association (SASTA, 6.3.4). To minimize turbidity, the juice sample was filtered through filter paper. The pH of the resultant solution was adjusted to 7.0 with 0.1 M NaOH. The Brix value was measured and converted into total dissolved solids (g ml^{-1}). The absorbance of the filtered solution was measured at 420 nm, and the ICUMSA color was calculated using eqn (9). This measurement is referred to as the ICUMSA 420 color, indicating that the color was measured at 420 nm.[40]

$$\text{ICUMSA Color(IU)} = \frac{\text{Abs} \times 1000}{w \times c} \quad (9)$$

where: Abs represents the absorbance of the solution at 420 nm, w is the cell width (1 cm), and c is the concentration of the diluted solution, equivalent to Brix (true density at 20 °C).

2.8.5. pH of the sample. The pH meter was calibrated with buffer solutions at pH 4, 7, and 10. After calibration, the sample was allowed to cool to room temperature before pH measurement. A prepared sugar sample weighing 10 grams was dissolved in an equal volume of water, and the resulting solution was used to determine pH. The pH measurements were conducted following a modified version of the Prada method, as referenced in the literature.[40]

2.8.6. Brix measurement of juice and sugar. The Brix degree, which indicates the sucrose content in an aqueous solution, was measured for both the raw and clear juices, as well as the prepared sugar, following the South African Sugar Technologists' Association (SASTA) method 6.1.8 *via* the refractometric approach.[39] The Brix value was subsequently determined directly using a refractometer calibrated at 20 °C.

2.8.7. Measurement of pol (%) and purity (%). The percentage of pol (%) in unclarified and clarified cane juices, as well as in sugar solutions derived from produced sugar, was measured using a digital polarimeter. This measurement aims to assess the concentration of sugar in the juices and in the raw sugar produced. The polarization of the juice and sugar solutions was measured at 20 °C using the D-line wavelength of the sodium lamp (589.3 nm). To ensure accuracy, the juice temperature was maintained at 20 °C by regulating the laboratory's external temperature throughout the experiment. The pol percentage at 20 °C was calculated using the following method:

$$\text{Percent pol juice} = \text{Measured Pol} \times \text{Pol factor of Brix} \quad (10)$$

$$\text{Juice or sugar purity (\%)} = (\text{Pol/Brix}) \times 100 \quad (11)$$

2.8.8. Moisture content of sugar. The moisture content (%) of the sugar was measured by assessing mass loss during drying, conducted in an air-forced drying oven (Model: MIDO/3/CLAD), following the methodology outlined in the literature.[39]

2.8.9. Ash content. The ash content of the sample was determined gravimetrically by dehydrating the sample (sugar) and then incinerating it in a furnace, with the process conducted in duplicate following the standard procedure.[40]

$$\text{Moisture(\%)} = \frac{\text{weight of sample} - \text{the weight of the oven} - \text{dried sample}}{\text{weight of the sample}} \times 100 \quad (12)$$

2.8.10. Determination of reducing sugar. Lane and Eynon's constant–volume titrimetric method for the ICUMSA standard GS1/3/7–3, 1994,[39] was used to quantify reducing sugars in the study samples. The amount of reducing sugar estimated in samples of raw juice, clarified juice, and prepared sugar,[40] is as follows:

$$\text{RS} = \frac{0.053 \times \text{Dilution factor(mL)}}{\text{Titer volume(mL)}} \times 100 \quad (13)$$

$$\text{Dilution factor} = \frac{\text{The final volume of solution after dilution}}{\text{The volume of an actual sample taken}} \quad (14)$$

where: 0.053 is Fehling's factor.

2.8.11. Boling house recovery. Maximizing sucrose recovery is a key goal for every sugar factory. The facility aims to enhance sucrose recovery at each step, from juice extraction to clarification. Nonetheless, even with efforts to reduce sugar losses

during processing, some losses can still happen, potentially resulting in financial challenges for the sugar mill.[41] The recovery of sugar during the processing of cane juice is referred to as boiling house recovery (BHR). This is determined by the ratio of sucrose extracted in the manufactured sugar to that present in the raw (unclarified) juice. The calculation follows eqn (15), as outlined:[41]

$$\text{Boiling house recovery} = (\text{Sucrose in sugar}/\text{Sucrose in raw juice}) \times 100 \quad (15)$$

2.9. Statistical analysis

Design-Expert (v.13.0.5.0, USA) was used to analyze the data. The ANOVA output for each response facilitated the identification of significant terms in the models. Significant factors were ascertained based on p-values, and the Tukey method was applied for mean comparisons. At a 95% confidence level, significant differences in mean values were identified ($p \leq 0.05$).

3. Results and discussion

3.1. Optimization of mixed fruit peels processing conditions

Optimizing the proportion of nano activated carbon derived from mixed fruit peels is essential to enhance its adsorptive properties for various applications, including water and wastewater treatment, dye effluent processing, and juice clarification in the food and sugar industries. This optimization process typically involves identifying the ideal activation conditions and the best combination of fruit peel types to achieve the desired surface area and adsorption capacity. For this study, maximizing the yield of fruit peel waste is critical for producing nano activated carbon (NAC), making it a key factor in selecting the raw material. The study indicated that chemical activation yields higher carbon output than physical activation.[29] Consequently, this study employed chemical activation with 40% H_3PO_4, which is expected to yield greater carbon and thus enhance NAC production.

This section focused on determining the optimal proportions of powdered fruit peel waste, with carbon yield as the dependent variable. The study investigates the impact of varying mixing ratios of peel powders on carbon yield. The independent variables, proportions of mixed peels, and the corresponding predicted and experimental yields are summarized in Table 1.

The experimental results closely align with the predicted values, indicating strong compatibility. As shown in Table 1, the carbonized matter yield from mixed peels (carbonized at 550 °C for 30 min) ranged from 66.05 ± 0.62% to 74.92 ± 0.34%. The carbon yield percentages from the experimental runs are statistically significant (p-value = 0.0019). Among the experiments, run 12, with a fruit peel proportion (g) of 13 : 43.5 : 43.5 (avocado, banana, and papaya, respectively), yielded the lowest carbon percentage at 66.05 ± 0.62%. In contrast, run 9, with a proportion (g) of 43.5 : 13 : 43.5, produced the highest carbon yield of 74.92 ± 0.34%.

This variation is likely attributed to the higher carbon content in avocado peels, which is 46.16 ± 0.32%,[42] surpassing that of banana and papaya peels at 39.08% and 50.8%, respectively, as reported in previous studies.[43,44] The findings suggested that the mixed peel waste used in this study yields higher carbon outputs than the individual peel wastes examined earlier, potentially due to the synergistic effects of the carbonized matter and the specific processing methods and conditions employed. Additionally, different fruit peels contain various forms of organic carbon, enhancing their biosorptive properties and improving the surface chemistry (*e.g.*, electrostatic attraction) of NAC, thereby contributing to significant waste reduction in actual waste treatment scenarios.[45]

The results were analyzed through analysis of variance (ANOVA), as detailed in Table S3. The model yielded an F-value of 512.50 and a corresponding p-value of 0.0019, which is lower than the 0.05 threshold, indicating that the regression model is statistically significant. This implies there is only a 0.019% probability that such a high F-value could arise from random noise. The linear variables (A, B, C) within the group showed significant differences, as evidenced by their low p-values ($p < 0.05$). Additionally, the interaction terms (AC and BC) also demonstrated significant differences ($p < 0.05$). The lack-of-fit F-value was 4.11 and non-significant, while the low pure error reflects the high precision of the experimental yield, as shown in Table S3. The non-significance of the lack-of-fit test suggests that the independent variables adequately account for the variability in the response variable.[46]

Moreover, this study assessed the model's goodness-of-fit using several metrics: the coefficient of determination (R^2), the adjusted R^2, the predicted R^2, the coefficient of variation (CV), and the signal-to-noise ratio (S/N). The high R^2 value of 0.9996 and adjusted R^2 of 0.9976, presented in Table 1, indicate a strong representation of the relationship between the response and independent variables, reflecting the model's high precision and reliability. The low CV value of 0.1676 further supports the consistency and reliability of the experimental results. The predicted R^2 of 0.9469 suggests only a 0.27% chance that the lack-of-fit F-value could result from noise. Furthermore, the predicted R^2 aligns well with the adjusted R^2, as the difference between them is less than 0.2. Adequate precision, which measures the signal-to-noise ratio, was 72.6031, indicating excellent model fit.[46]

3.1.1. Validation of the optimal proportions of MFP on carbon yield was also conducted. The study identified that carbon yield was significantly influenced by the three independent variables: avocado peel powder, banana peel powder, and papaya peel powder, all of which had a positive impact. A second-order polynomial model was developed to identify the optimal conditions for maximizing the NAC production. The desirability function method was employed to optimize these conditions, accounting for the desired response and determining the factor combination that maximizes overall desirability.[47] This analysis identified five optimal points

Table 2 Optimal proportions of fruit peels for the carbon yield were optimized using RSM

S. no	Avocado peel (g)	Banana peel (g)	Papaya peel (g)	Yield (%)	Desirability	
1	51.92	21.64	26.44	75.87	1.0000	Selected
2	50.80	20.20	29.00	75.64	1.0000	
3	49.80	29.40	20.80	75.56	1.0000	
4	50.00	19.40	30.60	75.40	1.0000	
5	49.30	24.70	26.00	75.37	1.0000	

(proportions of peel mixture) *via* numerical optimization, as shown in Table 2.

Among these five optimized conditions, the most favorable (sample number 1) included mixture of avocado, banana, and papaya peels of 51.92 g, 21.64 g, and 26.44 g, respectively, with a carbon yield of 75.87% and a desirability value of 1.0000. This desirability score indicates that the model developed for predicting carbon yield is highly accurate and desirable.

3.2. Optimization of processing conditions for the synthesis of NAC using mixed fruit peels by the quadratic regression model

Generally, the combined nature of avocado, papaya, and banana peels enriches NAC with diverse lignocellulosic and mineral compositions, generating hierarchical porosity and varied functional groups. This synergy enhances surface reactivity, adsorption capacity, and structural stability, yielding a more efficient, selective, and sustainable nano activated carbon compared to single-biomass precursors.

The optimization of various parameters, treated as independent variables, included the impregnation ratio (with 1–2 levels of the MFP activating agent and H_3PO_4), carbonization temperature (ranging from 400 to 700 °C), and heating time (40–100 min). This optimization process, detailed in Table 3, aimed to achieve optimal conditions for NAC synthesis, resulting in high fixed carbon content and surface area.

The results presented in Table 3 were analyzed using the Response Surface Methodology with a Central Composite Design (RSM-CCD), as implemented in Design-Expert software (v.13.0.5.0, USA). The analysis showed significant variations in the responses ($p < 0.05$), as indicated in Table 3.

In experimental run two, the highest fixed carbon content (81.44 ± 0.43%) and surface area (565.44 ± 0.50 $m^2\ g^{-1}$) were observed, achieved with a 33.3 : 66.7 impregnation ratio (%), a carbonization temperature of 400 °C, and a carbonization time of 100 minutes. Conversely, the lowest fixed carbon content and surface area, 60.50 ± 0.6% and 143.08 ± 0.04 $m^2\ g^{-1}$, were recorded in runs 3 and 6 under different experimental conditions, as detailed in Table 3.

The results process parameters, including interaction effects, were analyzed using variance analysis (ANOVA), with findings presented in Table S4. The model *p*-values for the

Table 3 Results of independent and dependent variables, and ANOVA summary on optimization of NAC synthesis from mixed fruit peels using RSM[a]

	Independent variables			Dependent variables	
Run	Impregnation ratio (%)	Temperature (°C)	Time (min)	Fixed carbon contents (%)	Surface area ($m^2\ g^{-1}$)
1	33.3 : 66.7	700	100	76.61 ± 0.53^{c}	390.02 ± 0.40^{e}
2	33.3 : 66.7	400	100	81.44 ± 0.43^{a}	565.44 ± 0.50^{a}
3	50 : 50	700	40	60.50 ± 0.60^{f}	224.66 ± 0.40^{i}
4	50 : 50	400	70	80.20 ± 0.50^{a}	320.03 ± 0.79^{f}
5	25 : 75	550	70	78.54 ± 0.52^{b}	409.45 ± 0.39^{c}
6	40 : 60	550	70	68.30 ± 0.20^{d}	143.08 ± 0.04^{j}
7	25 : 75	338	70	65.36 ± 0.60^{e}	290.07 ± 0.51^{g}
8	25 : 75	762	28	68.09 ± 0.70^{d}	240.44 ± 0.43^{h}
9	25 : 75	550	112	68.51 ± 0.40^{d}	393.48 ± 0.51^{d}
10	25 : 75	550	70	78.16 ± 0.60^{b}	408.54 ± 0.41^{c}
11	25 : 75	550	70	78.26 ± 0.60^{b}	408.84 ± 0.41^{c}
12	25 : 75	550	100	77.85 ± 0.40^{bc}	443.02 ± 0.41^{b}
ANOVA summary: regression coefficient, R^2				0.9956	0.9958
Adj. R^2				0.9941	0.9943
Pre. R^2				0.9914	0.9933
CV%				0.702	2.68
Adeq. precision				78.3959	87.1136

[a] Triplicate experiments were performed ($n = 3$). All values are presented as mean ± standard deviation; mean values (in the column) with different superscripts are significantly different ($p < 0.05$).

responses of fixed carbon content (FCC) and surface area (SA) were 0.0008 and 0.0103, respectively, indicating statistical significance and revealing insights into interaction patterns.[48,49] Notably, interaction terms (AB, AC, and BC) demonstrated significance with p-values below 0.05 for both FCC and SA, as shown in Table S4.

The model F-values for FCC (1227.41) and surface area, SA (96.15) suggested that the quadratic model employed is significant. A high F-statistic coupled with a low p-value indicates that the regression model is likely statistically significant, suggesting a good fit for the data and a significant relationship between the independent and dependent variables. Table S4 illustrated that the F-values for most linear interactions and quadratic terms were notably high, with p-values below 0.05, suggesting the model equation effectively explains the responses.[48,49]

However, the term A (impregnation ratio) was found to be non-significant (p-value = 0.3237) for FCC, whereas in the case of SA, terms A (p-value = 0.2754) and B^2 (p-value = 0.2261) were also non-significant. The model's pure error was minimal (zero), reflecting the high precision of the experimental results for both fixed carbon content and surface area. This is further supported by the significant F-value for carbonization time (1268.59 for FCC), which was substantially greater than that for SA (64.64), as shown in Table S4, with temperature and impregnation ratio following in significance.

The results in the graphs shown in Fig. 1a and b are plotted between this study's predicted and actual values. Indicates that the actual values are distributed near the straight line, confirming the model's better fit to the experimental data. Furthermore, the results were found to be adjacent for FCC and SA. Thus, the study reveals the lowest deviation and competent agreement between the tangible and predicted data.

Fig. 1c and d describe the plots of the internal Studentized residuals *versus* the experimental runs. These plots are used to check the fit of the developed model to the experimental data. As shown in Fig. 1c and d, all data points were within the

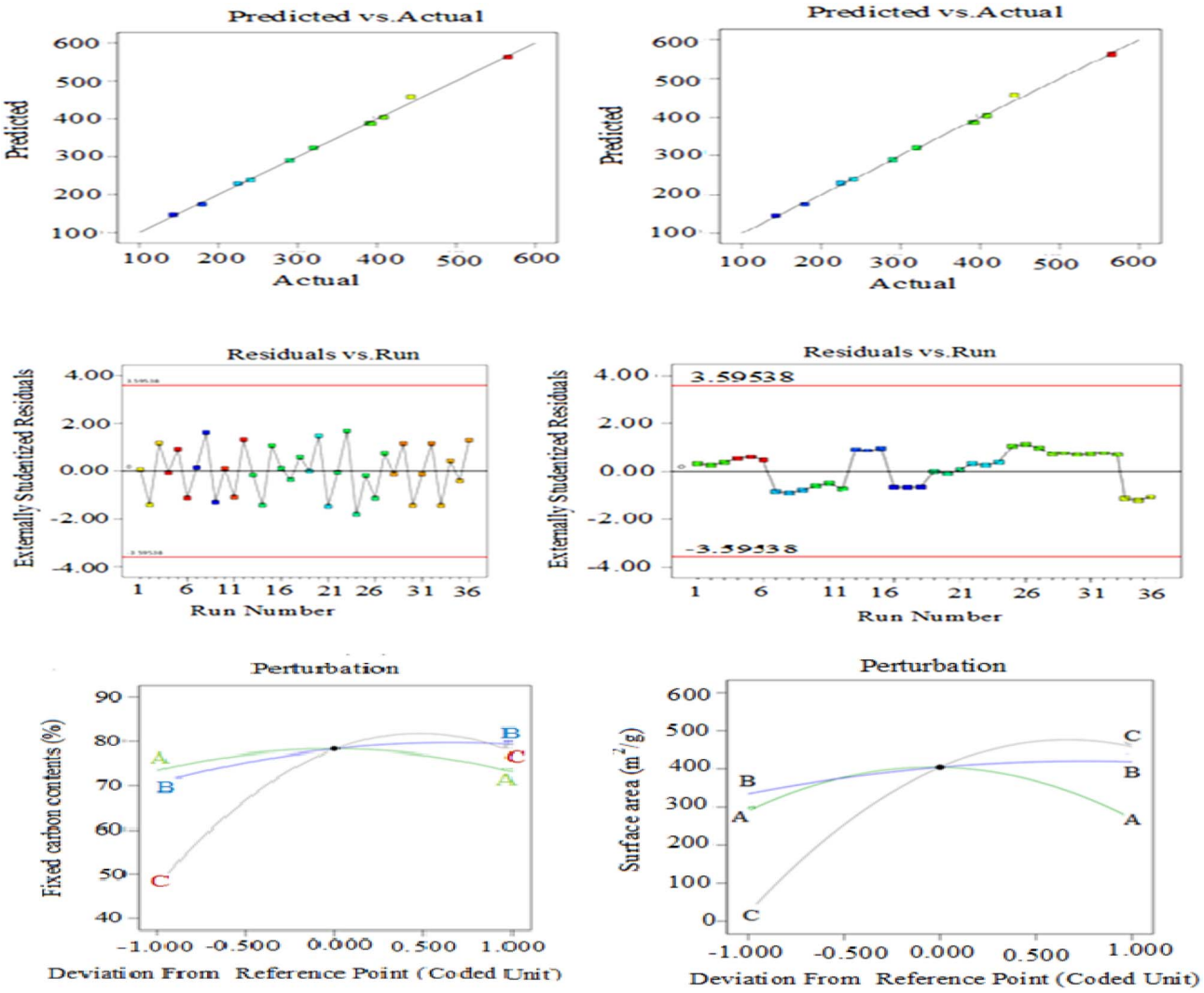

Fig. 1 Processing optimization plots for the preparation of NAC from MFPs: Predicted *vs.* actual results of fixed carbon content (a) and surface area (b); diagnostic plots for adequacy of developed model for FCC (c) and SA (d); perturbation plots to show the effect of operational parameters on FCC (e) & SA (f).

allowable permissible limits (−2 to +2). However, the higher limit suggested for the model (−3.59538 to +3.59538, as shown in Fig. 1c and d). The results show that the developed model fits the experimental data well.[50]

The perturbation plot was used to identify the most influential independent variables in the responses. The comparative influence of the studied factors on %FCC and SA at a particular design point is shown in the perturbation plot in Fig. 1e and f. In the current study, the carbonization time (factor *C*) primarily influences the percentage of fixed carbon and the surface area, more than the carbonization temperature and the impregnation ratios. It is revealed that the slope of the carbonization time curve is the steepest, as shown in Fig. 1e and f. In contrast, the slopes of the other independent variables in the perturbation plot are flatter, confirming that factors *A* and *B* are less significant.

In a comparative analysis, the interaction term BC outperformed the other interaction terms, AB and AC. It showed a higher NAC surface area (600 $m^2\ g^{-1}$) and a higher fixed carbon content (>80%) at lower temperatures. The *F*-values for the interaction terms also corroborate this, with BC yielding higher *F*-values (FCC: 4589.93 and SA: 131.63) across both responses compared to AB and AC, as demonstrated in Table S4. Consequently, the optimized processing parameters and the evaluated responses for NAC synthesis align closely, indicating that the interaction term BC is particularly effective.

3.3. Validation of optimal conditions for MFP-NAC synthesis

Using Design-Expert software (v.13.0.5.0, USA), numerical optimization for maximum desirability was conducted to optimize the independent variables (impregnation ratio, carbonization temperature, and carbonization time) for the responses of FCC and SA. Based on the desirability values and the elevated levels of FCC and SA, four optimal experimental conditions were selected, as shown in Table 4. Among the four experimental runs listed in Table 4, the optimal conditions (optimized sample 1) identified were an impregnation ratio (%) between MFP and acid ratio 38.5 : 61.5, a carbonization temperature of 409.9 °C, and a carbonization time of 100 minutes, yielding a fixed carbon content of 89.63% and a surface area of 620.71 $m^2\ g^{-1}$, achieving a unit desirability value.

The optimal process variables identified in Table 4 are clearly demonstrated and validated by the desirability contour plots in Fig. 2. The analysis indicated that the predicted FCC yield is 89.63% and the surface area is 620.71 $m^2\ g^{-1}$, which align with the best-optimized conditions for producing NAC. To verify the appropriateness of the selected optimized conditions (impregnation ratio: 38.5 : 61.5; carbonization temperature: 409.9 °C; carbonization time: 100 min), experiments were conducted in triplicate. The results showed a fixed carbon content of 89.25 ± 0.38% and a surface area of 650.87 ± 0.26 $m^2\ g^{-1}$, which closely matched the software's predictions.

The reproducibility of the mixture of peels described as the use of mixed fruit peels (avocado, banana, and papaya) introduces compositional variability due to differences in lignin, cellulose, and ash content. However, reproducibility is ensured through: (i) controlled mixing ratios optimized *via* RSM, (ii) standardized preprocessing (drying, grinding, sieving), and (iii) fixed activation conditions. Although minor variability between fruit batches may occur, the strong statistical agreement between predicted and experimental values (R^2 = 0.9996) confirms high reproducibility. Additionally, synergistic interactions among the different peel types enhance consistency in adsorption performance compared to single-source biomass. This also demonstrates the robustness of the method against batch-to-batch variability due to process optimization.

3.4. Physicochemical properties of MFP and NAC

Analyses of raw materials (MFP) and synthesized NAC were conducted to evaluate several physicochemical characteristics, including moisture, volatile matter, ash, and fixed carbon content of the optimized NAC, as shown in Table 5. Additionally, the percentage yield of synthesized NAC, the point of zero charge, and the surface area were assessed.

3.4.1. Moisture content. The moisture content reported in Table 5 reflects the hygroscopic nature of carbon, indicating its capacity to absorb moisture. The moisture levels of both the raw material (MFP) and the optimally designed, processed NAC were measured. The findings revealed that the moisture content for MFP was 4.62 ± 0.03%, while NAC exhibited a lower level at 3.43 ± 0.32%. This reduced water retention in the prepared materials suggests that NAC has a lower moisture content than MFP, primarily because of the carbonization and activation processes applied to the raw materials in this study. Consequently, NAC's lower moisture content makes it a suitable adsorbent for removing impurities from aqueous solutions. The reduced moisture content indicated that little water was present on the surface of the activated carbon, enhancing its effectiveness as an adsorbent.[51]

3.4.2. Ash content. The raw material (MFP) and the prepared NAC exhibited ash contents of 11.23 ± 0.26% and 4.38 ± 0.48%, respectively, as shown in Table 5. The lower ash

Table 4 The software identified the four best-optimized conditions and responses (per cent fixed carbon content and surface area) for preparing NAC from mixed fruit peels

S. no.	Impregnation ratio (%)	Temperature (°C)	Time (min)	Fixed carbon contents (%)	Surface area ($m^2\ g^{-1}$)	Desirability	
1	38.5 61.5	409.9	100	89.63	620.71	1.0000	Selected
2	38.8 61.2	401.4	98	89.54	613.57	1.0000	
3	38.3 61.7	403.9	97	89.04	611.42	1.0000	
4	37.6 62.4	409.5	98	87.24	606.59	1.0000	

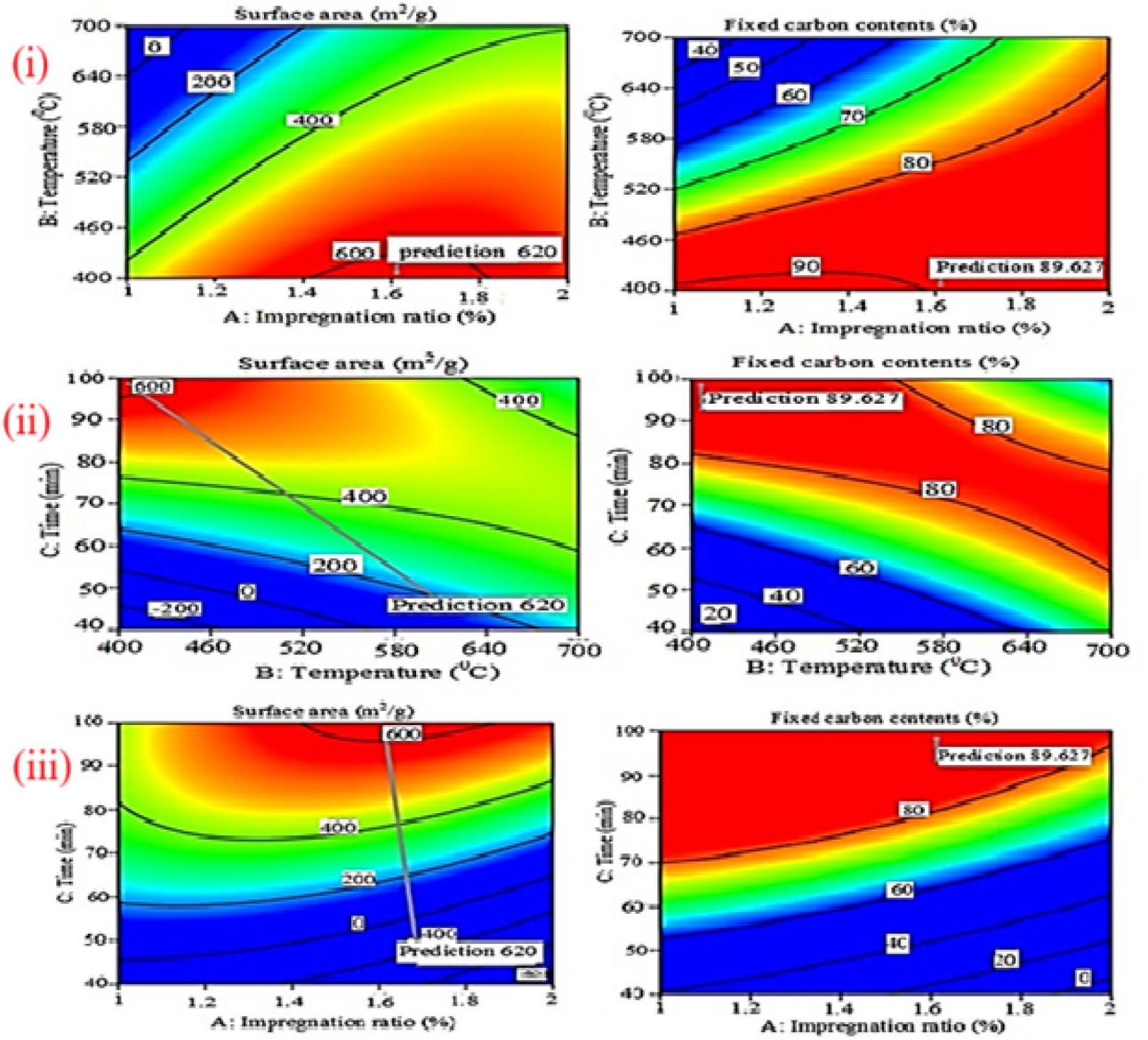

Fig. 2 The contour plots for the best-optimized variables of the interaction terms AB (i), AC (ii), and BC (iii) of the surface area and fixed carbon contents were obtained to prepare NAC.

Table 5 Physicochemical properties of mixed fruit peels (avocado, banana, papaya) and NAC[a]

	Obtained results	
Parameters (%)	Raw material, MFP	Prepared NAC
Moisture	4.62 ± 0.03[a]	3.43 ± 0.32[b]
Ash	11.23 ± 0.26[a]	4.38 ± 0.48[b]
Volatile content	73.89 ± 0.06[a]	4.94 ± 0.05[b]
Fixed carbon content	10.28 ± 0.11[b]	89.25 ± 0.38[a]
The yield of NAC (%)	—	74.86 ± 0.01
Surface area (m^2 g^{-1})	—	650.87 ± 0.26

[a] Data expressed as means ± standard deviation of triplicate experiments (n = 3). Mean values within the same row that have different superscripts indicate statistical significance (p < 0.05). NAC refers to NAC.

content in MFP indicates a lower inorganic content, making it an ideal precursor for NAC production. The reduced ash content in NAC likely results from the removal of most inorganic matter during carbonization and activation. Furthermore, during NAC washing, soluble ashes are separated and removed, yielding a product with minimal ash content (and thus low inorganic material). This characteristic is essential for effectively clarifying cane juice and eliminating pollutants from wastewater. Typically, the most effective NAC is derived from materials with the least ash content.[52] A high ash concentration indicated lower NAC quality, as it can leach into the sugar solution during clarification, compete with carbon adsorption, and lead to undesirable reactions.[52]

3.4.3. Volatile matters. The volatile matter content indicates the presence of non-carbonaceous components. The

studied MFP's carbon-rich biomass feedstock exhibited a high volatile organic content of 73.89 ± 0.06%. As shown in Table 5, the elevated volatile matter content makes the raw material an outstanding precursor for the synthesis of nano activated carbon (NAC). The volatile matter from the raw material is transformed into NAC by the breakdown of its organic content, facilitated by the hydrolytic activity of the activating agents, followed by carbonization in a muffle furnace at 950 °C for 7 min. During this decomposition, volatile components, primarily hydrogen, oxygen, and nitrogen, are released from the carbonaceous product.[53] Given that NAC has a low volatile matter content of 4.94 ± 0.05%, it may be an effective clarifier for purifying sugarcane juice and treating wastewater.

3.4.4. Fixed carbon content. Fixed carbon refers to the residual amount present in a substance after it has been exposed to high temperatures. During carbonization, carbon-rich raw materials do not form porous carbon, which is advantageous for adsorption purposes.[54] Table 5 presents the fixed carbon content of MFP and NAC, recorded as 10.28 ± 0.11% and 89.25 ± 0.38%, respectively. The results indicate that the fixed carbon content of the synthesized NAC is significantly higher than that of MFP. This difference may be attributed to the quantities of cellulose and lignin that can be converted into carbon atoms, which also affects the fixed carbon content. The high fixed carbon levels observed in this study suggest that NAC could serve as a valuable material for applications such as clarifying sugarcane juice and beverages, as well as for removing pollutants in wastewater treatment, among other uses.

3.4.5. Percentage of NAC yield. The quantity of residual original material remaining after pyrolysis is referred to as the NAC yield. In this study, the NAC yield was 74.86 ± 0.01% under the optimal process conditions outlined in Table 7, including carbonization and MFP activation. Thus, any carbon-based material can be incinerated, releasing a considerable amount of volatile substances and forming tiny internal cavities, or pores. The capacity of NAC to absorb both organic and inorganic materials from liquids or gases is significantly enhanced by the high surface area relative to its weight. Compared with the literature, the current yield of NAC (74.86 ± 0.01%) was higher than the reported values (0.20–0.35 kg NAC per kg dry peels).[55,56]

3.4.6. Specific surface area of the prepared NAC. Factors such as surface area and surface chemistry play a crucial role in the adsorption of impurities from liquid media, such as sugar liquor.[54] An effective adsorbent typically possesses a large surface area. For optimal adsorption of the target species, it is essential to have an appropriate distribution of pore sizes and surface chemistry. Under the best-optimized conditions, the surface area was measured at 650.87 ± 0.26 $m^2 g^{-1}$, as indicated in Table 4. An observed that low clarification efficiency was primarily due to a limited surface area (ranging from 78 to 180 $m^2 g^{-1}$) in activated carbon derived from sugarcane bagasse, coal tar, and a mixture of sugarcane bagasse and corn syrup.[57] In contrast, the combination of sugarcane bagasse and corn syrup produced granular activated carbons (GACs) with a moderate surface area (300 $m^2 g^{-1}$), a favorable pore-size distribution, and a relatively low surface charge, which contributed to their effective sugar clarification. They reported that a high specific surface area of 613.89 $m^2 g^{-1}$ facilitates the easy penetration of colored organic compounds into the internal surface of PACW.[58] Compared to these findings, the currently synthesized NAC from mixed fruit-peel demonstrates a large surface area, which may enhance its ability and confirm its suitability to adsorb pollutants and for aqueous system clarification, as they indicate extensive microporosity, high adsorption capacity, and strong affinity for small dissolved pollutants, supported by the literature.[59] Consequently, iodine-derived estimates serve as a reliable and practical tool for assessing the performance of nano activated carbons in water and wastewater applications.[60]

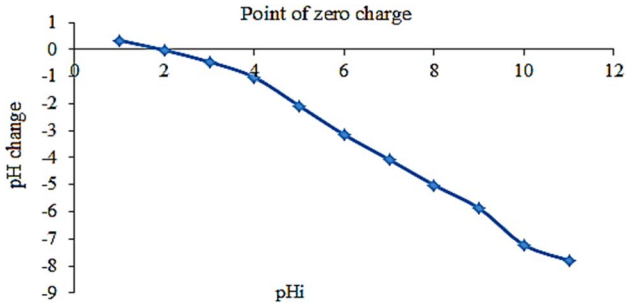

Fig. 3 The point of zero charges of NAC prepared from mixed fruit peels.

3.4.7. Point of zero charge. The clarification or adsorption capacity of a surface, along with its active surface centers, is quantified by a critical parameter known as the point of zero charge (pHpzc). The electrostatic properties and surface charge of the NAC were assessed using this point, which signifies the pH at which the surface charge is neutral. This measurement is essential for evaluating the electrokinetic activity of both adsorbents and adsorbates. Determining the pHpzc is crucial for understanding how pH affects adsorption and the surface behavior of the synthesized NAC. In this study, the point of zero charge (pH_0) of NAC was investigated over a pH range of 1–12 to determine the pH at which the surface charge becomes zero. The pHpzc was determined by plotting the initial pH (pH_i) against the change in pH. As illustrated in Fig. 3, the zero-charge point was found to be 2.01.

At pH values below the pHpzc (pH < 2.01), the NAC surface carries a positive charge due to the high concentration of H^+. This condition enhances the adsorption of anionic impurities, organic molecules, and colorants from aqueous solutions, such as cane juice, beverages, and wastewater, due to increased electrostatic attraction. Conversely, at pH values above the pHpzc (pH > 2.01), the NAC surface becomes negatively charged, leading to competition with positively charged cations present in the solution. This competition can fill the adsorbent's available adsorption sites, reducing the uptake of contaminants from polluted aqueous media.

3.5. Characterization of MFP and NAC

3.5.1. FTIR spectroscopic study of MFP and NAC's. A spectroscopic analysis (FTIR) was conducted to identify the

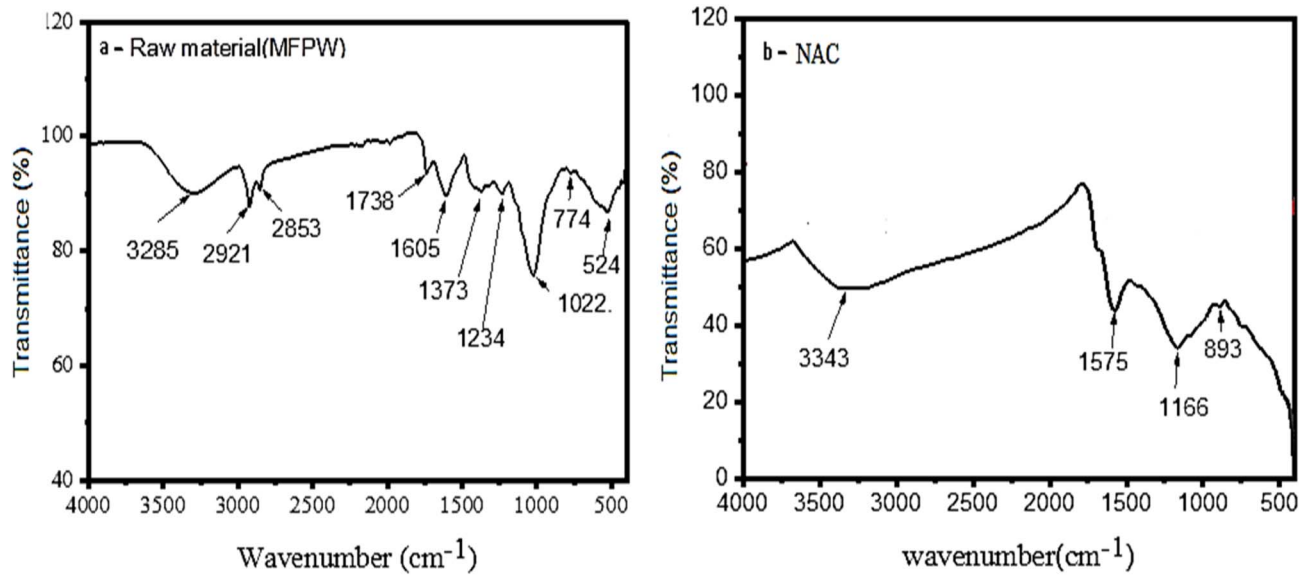

Fig. 4 FTIR spectrum of mixed avocado, banana, and papaya peel powder (a), and NAC prepared from the mixed fruit peel powder under optimized process conditions (b).

functional groups present in the mixed fruit peels (MFP) and NAC, as illustrated in Fig. 4a and b.

3.5.1.1. FTIR analysis of MFPs. Fig. 4a illustrates the FT-IR spectrum of MFP, which displays notable bands at 3285 cm^{-1}, 2921 cm^{-1}, 2853 cm^{-1}, 1738 cm^{-1}, 1605 cm^{-1}, 1373 cm^{-1}, 1234 cm^{-1}, 1022 cm^{-1}, 774 cm^{-1}, and 524 cm^{-1}. The broad band around 3285 cm^{-1} corresponds to O–H stretching, indicating the presence of alcoholic and phenolic –OH functional groups in MFP.[61]

The bands at 2921 cm^{-1} and 2853 cm^{-1} represent a doublet of C–H stretching ($-CH_2$) groups, reflecting symmetric and asymmetric stretching modes typically associated with carbohydrates (polysaccharides) and lipids.[62] The bands observed at 1738 cm^{-1}, 1605 cm^{-1}, and 1373 cm^{-1} are attributed to C=O stretching of aldehydes or carboxylic acids (–COOH), asymmetric stretching of carboxylic C=O, and O–H bending, respectively.[63,64] Additionally, the band at 1234 cm^{-1} is indicative of aromatic C=C stretching.[65] The peaks at 524 cm^{-1} are linked to Si–O stretching and Si–O bending, signifying the presence of silica.[66] The band at 1022 cm^{-1} is associated with C–N and C–O stretching from alcohol and lignin. In the fingerprint region (1200–800 cm^{-1}), characteristic symmetric stretching bands of typical carbohydrates, including C–C, C–OH, and C–O–C groups, are revealed.[67]

3.5.1.2. FTIR analysis for NACs. The FTIR spectra of MFP and NAC, as presented in Fig. 4a and b, reveal notable differences. It appears that certain functional groups are diminished in NAC, which is derived from MFP *via* carbonization and phosphoric acid activation at elevated temperatures. Additionally, the carbonization and activation process leads to the release of less stable volatile compounds, primarily oxygen-containing derivatives, thereby increasing the spacing between carbon atoms.[68] In Fig. 4b, the most prominent and broad peak at 3343 cm^{-1} corresponds to the stretching vibrations of hydroxyl (–OH) groups associated with alcohols, adsorbed water, and phenols. The lignin component, which possesses an aromatic structure, undergoes degradation and is reconfigured into various compounds featuring C=C bonds in NAC.[25] As depicted in Fig. 4b, the strong and pronounced peak at 1575 cm^{-1} signifies the presence of C=C bonds, while the broad peak at 893 cm^{-1} is attributed to nitrogen-containing bioligands, as corroborated by existing literature.[64]

Overall, the FTIR spectra indicate that the acid oxidation process enhanced the NAC surface by increasing the number of oxygen-containing functional groups, such as carboxyl and hydroxyl groups. These functional groups can bind charged ions *via* biosorption. The FTIR analysis further indicates that NAC derived from MFP is rich in hydroxyl and carboxylic groups, likely originating from hemicellulose, cellulose, lignin, and amines.[69] These functional groups (–COOH, $-NH_2$, –OH, *etc.*) on the adsorbent's surface can form hydrogen bonds with other molecules, facilitated by the attractive electrostatic interactions between the hydrogen atoms in these functional groups. This characteristic allows the NAC to attract and bind negatively charged impurities and activated carbon.

3.5.2. XRD analysis for MFP and NAC. X-ray diffraction (XRD) is a highly adaptable, non-destructive analytical technique used to identify and quantitatively assess crystalline forms in powdered and solid samples.[30] It has been observed that crystalline materials exhibit distinct peaks in their diffraction patterns, whereas non-crystalline materials show a more diffuse pattern without well-defined peaks.

In this study, Fig. 5a and b illustrate the XRD patterns for MFP and NAC, respectively. The XRD pattern of the precursor MFP in Fig. 5a showed peaks that suggest an amorphous character of the raw materials. The cellulose XRD pattern, shown in Fig. 5a, exhibits well known diffraction peaks at approximately 16.5° and 22.5°, corresponding to the (110) and

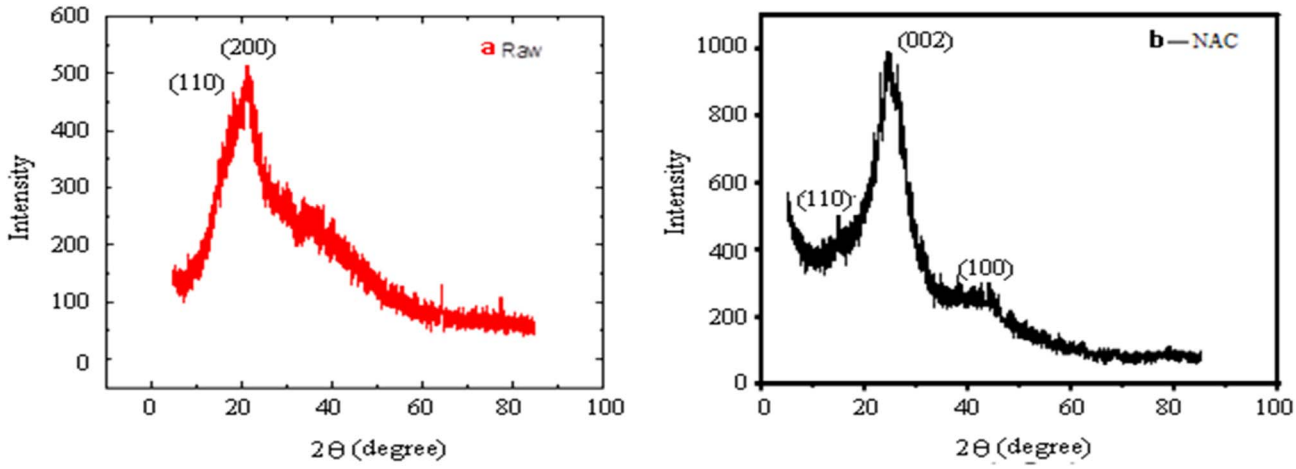

Fig. 5 The XRD pattern of raw MFP (a) and synthesized NAC (b) from MFP.

(200) planes, respectively. These findings aligned with the characteristic diffraction peaks expected for cellulose, attributable to the heterogeneous composition of MFP, which includes complex matrix components like proteins, lipids, and carbohydrates.

The analysis revealed that both strong and weak diffraction peaks at $2\theta = 24.28°$ and $2\theta = 44.3°$, corresponding to interplanar spacings D 002 and D 100, respectively, indicate the presence of graphite crystallites within the activated carbon derived from peel.[70] Additionally, a prominent peak at $2\theta = 24.28°$ is noted in Fig. 5b, suggesting the partially crystalline nature of the synthesized NAC.[11] This transition is likely due to the carbonization process, during which the sample is subjected to high temperatures, leading to the loss of its amorphous characteristics as most organic components are eliminated.[69,71] The crystalline size of the synthesized NAC was determined using the standard material shape tool in ImageJ, yielding an average crystalline size of 24.46 nm.

Further, the effectiveness of the activated carbons obtained from mixed fruit peels, supported by literature,[23,72] accordingly, prepared NAC typically exhibits turbostratic carbon, characterized by randomly oriented, poorly stacked graphene layers that generate broad (002) and (100) XRD reflections and enlarged interlayer spacing compared with crystalline graphite. This disorder arises from biomass heterogeneity and chemical activation, which disrupt aromatic-layer alignment and promote defect-rich, porous structures favorable for adsorption. However, crystalline sizes estimated using the Scherrer equation are only semi-quantitative for such materials, as peak broadening also reflects lattice strain, rotational disorder, and amorphous content rather than true domain size alone.[23,73]

3.5.3. Scanning electron microscopic analysis of MFP and NAC. In this study, scanning electron microscopy (SEM) was used to examine morphological modifications in mixed fruit peel (MFP) and synthesized NAC. Fig. 6a and b show SEM images of MFP and NAC at magnifications of ×1500 and ×3000, respectively. Before chemical modification, the raw MFP exhibited a heterogeneous surface, as depicted in Fig. 6a. After modification, the NAC displayed significant changes, characterized by a porous texture with deep holes and a distinct pattern. The increase in NAC's specific surface area is likely due to carbonization at elevated furnace temperatures, coupled with oxidation of raw MFP using H_3PO_4. Generally, acid treatment of an adsorbent can enhance its capacity to adsorb other molecules by altering its surface properties, such as increasing ion-exchange capacity, introducing new functional groups, or creating additional active binding sites.[74]

The SEM image of NAC in Fig. 6b shows numerous irregularly shaped pores, which is advantageous because they provide a larger surface area for adsorption. The activated carbon produced in this study exhibits a morphology comprised of nano-sized spherical particles distributed across its surface, with an average particle diameter of 24.46 nm, as indicated in Fig. 6b. This finding aligns with the observations made in earlier,[74] who noted that chemical and thermal modifications impact the surface morphology of activated carbon. Additionally, this research builds upon previous findings reported,[75] which demonstrated that cellulose-based materials can yield activated carbon with irregular (amorphous) and non-uniform particle structures, including nano-sized particles. Thus, the activated carbon examined here is confirmed to be nanoscale.

Additionally, the particle size distributions of MFP and NAC are illustrated in Fig. 6. The particle size distribution of activated carbon was estimated using ImageJ software, assuming irregular particle shapes. This distribution was calculated from particle areas, following the methodology outlined.[76] The particle size distribution for MFP ranged from 0 to 300 μm, while that for NAC ranged from 10 to 60 nm, as depicted in Fig. 7a and b, respectively. The peak particle sizes for MFP and NAC were observed at 50–100 μm and 20–30 nm, respectively. These findings were further validated by the SEM images presented in Fig. 6. Based on SEM analysis, the researchers inferred the particle size distributions of the samples. They plotted the corresponding curves in Fig. 7. The average MFP diameter was determined to be 64.66 μm. At the same time, MFP-NAC in Fig. 7b exhibited a range of surface areas and an average particle

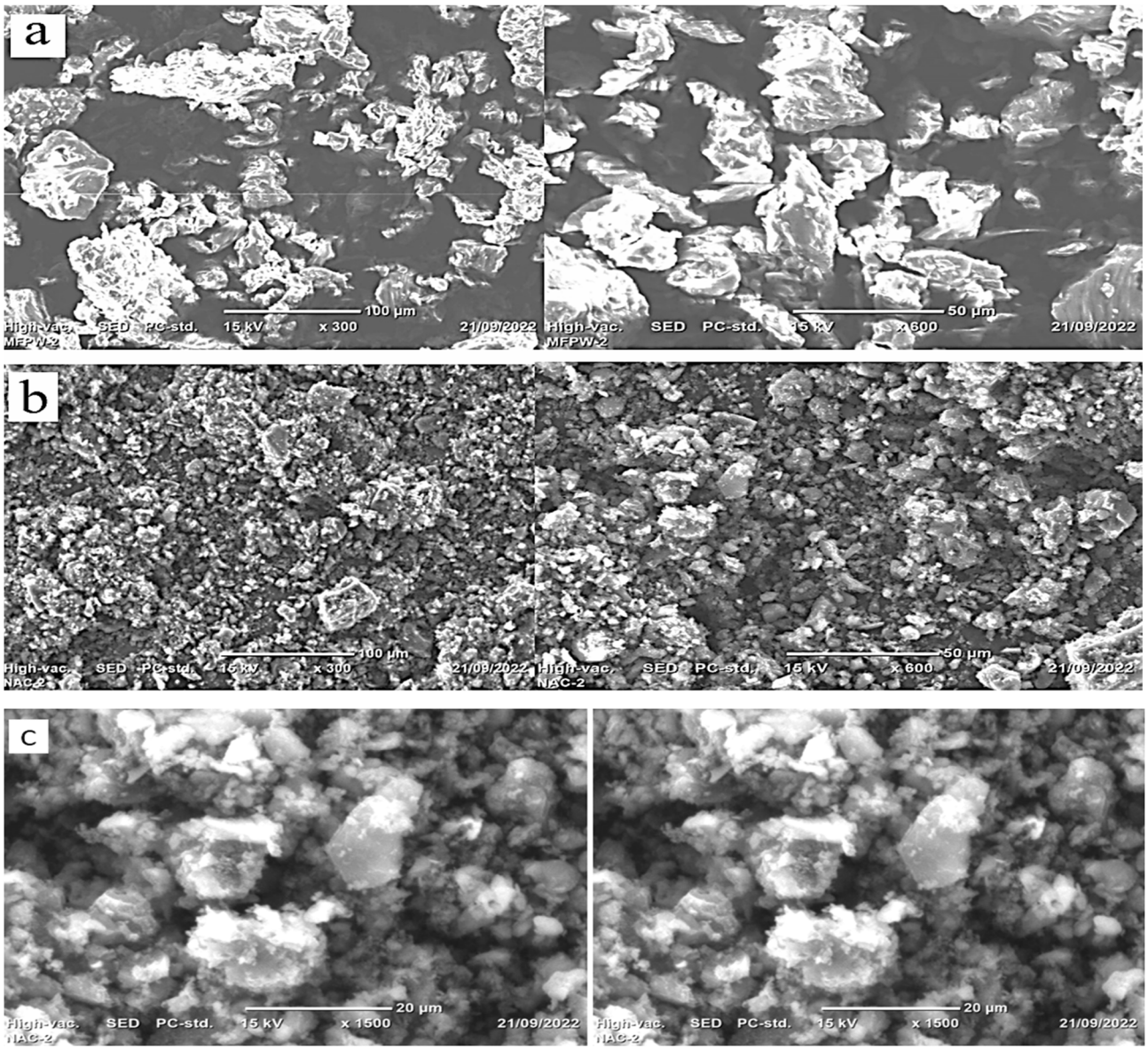

Fig. 6 SEM image of raw MFP (a) and synthesized NAC before clarification (b), and after clarification (c) at different magnifications.

size of 24.46 nm. This difference is attributed to the treatment of MFP with phosphoric acid, pyrolysis, and grinding.

The results of this study on nano activated carbon can be compared with those of similar research, as summarized in Table 6. According to the current study, the nano activated carbon produced exhibits impressive characteristics, with a specific surface area of 650.71 $m^2\ g^{-1}$ and a nanoparticle size of 24.46 nm. These measurements are favorable compared with those reported for activated carbon derived from fruit peel waste in related studies that employed low-temperature physical and chemical activation methods. Moreover, the approach taken in this study is both cost effective and environmentally friendly, as it avoids the use of chemical reagents and utilizes mixed fruit peel waste, a type of market waste, as the precursor. One significant and expanding application of activated carbon, particularly in its nano-sized form, is its effectiveness as an adsorbent. As such, the nano activated carbon produced in this study has the potential to efficiently remove heavy metals, dyes, and various organic pollutants or impurities from aqueous solutions.[9,25,28,29,56,64,77]

3.5.4. Acid recovery and wastewater generation. Furthermore, the study was undertaken on washing load for phosphoric acid recovery to assess the mass balance and environmental impact. The study used 4.2 L kg^{-1} of NAC in water during NAC preparation from mixed fruit peel wastes, using phosphoric acid activation. The washing step generates a moderate acid recovery/washing load, as excess acid and phosphate species must be removed to neutral pH. Typically, a wash water of 3–6 L per kg of carbonized material is a reasonable, often conservative, estimate for removing chemical residues and washing until neutrality, particularly when acid recovery or recycling is involved.[78]

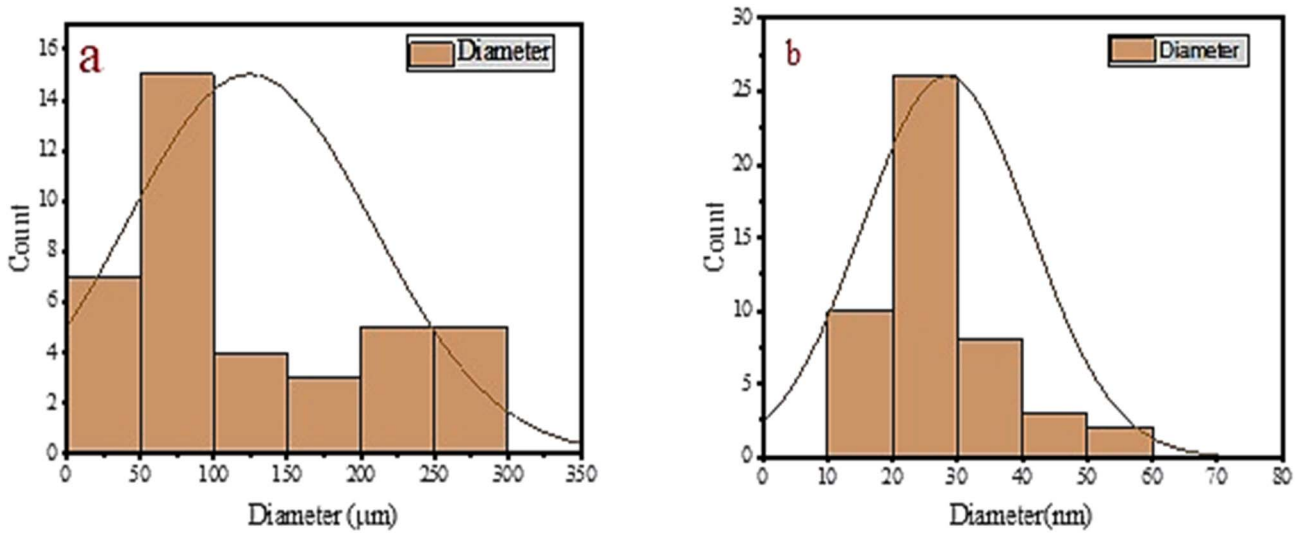

Fig. 7 Size distribution of MFP (a) and NAC (b), with an average particle size of 64.66 μm and 24.46 nm, respectively, using Image J software.

In the preparation of nano activated carbon (NAC) from mixed fruit peel wastes using phosphoric acid activation, wastewater is mainly generated during the post-activation washing step. This effluent contains residual H_3PO_4, dissolved organic matter, and phosphate ions, with volumes typically proportional to the pH-neutralization requirements of the wash. Proper treatment or reuse is necessary to minimize environmental impact.

3.5.5. SEM analysis of NAC after cane juice clarification. SEM micrographs of NAC, presented in Fig. 6c, reveal a significant alteration in the surface texture of NAC following clarification. The NAC surface, now loaded with impurities, indicates that non-sucrose components have obscured the adsorbent surface. Post-adsorption, the pores appear filled with these impurities, resulting in a smoother surface. This smoothing effect may be attributed to a reduction in the adsorbent's surface heterogeneity.

The NAC surface coverage likely results from the adsorption of non-sugar molecules from cane juice, potentially forming a uniform monolayer. This is evidenced by the appearance of a white layer (referred to as a molecular cloud) of consistent thickness and spread, as observed in the SEM image of NAC used for cane juice clarification in Fig. 6c. This observation aligns well with previous literature.[77] Fig. 6c highlights the significant changes on the NAC surface, indicating that impurities have been adsorbed onto functional groups within the

Table 6 Comparisons of the results for the surface area of NAC obtained in the present study with those reported in the literature for activated carbon from different sources of fruit peel waste

Raw material	Activating agents	Surface area ($m^2\ g^{-1}$)	Applications	References
Annatto peel	H_3PO_4	Not reported	—	9
Banana peel	$ZnCl_2$	Not reported	Reducing the air pollutants (mainly CO) from the motorcycle muffler	25
Lemon/citrus peel	$ZnCl_2$/KOH	850–1100	Water purification	56
Avocado peel	—	87.52	Removal of naphtha blue black, reactive black 5 dye, and basic blue 41 dye	28
Orange peel	$ZnCl_2$	1228.2	Removal of 99.12% Cr(VI) from aqueous medium	29
Papaya peel	1 M H_3PO_4	—	Removal of Pb^{2+} from aqueous medium	64
Pineapple peel	H_3PO_4/KOH	850–1200	Aqueous dye adsorption	77
Mixed peels: banana + papaya + avocado peels	H_3PO_4	650.87 ± 0.26	Prepared nano activated carbon can be used as an adsorbent to remove dyes, heavy metals, and other organic impurities from aqueous media, reduce CO gas emissions*etc.*	Present study

pores, a finding further supported by FTIR analysis following cane juice clarification, as shown in Fig. 6b using NAC as the adsorbent. Additionally, the pores on the NAC surface appear to be blocked, with the adsorbent particles aggregating. After the clarification process, the average particle diameter of NAC increased to 45.12 nm, as shown in Fig. 6c. This increase can be attributed to NAC's tendency to agglomerate, consistent with previous studies.[30]

3.6. Yield of sugarcane juice

The quality of the sugarcane and the efficiency of the juice extraction process significantly influence the juice yield. High-quality cane typically has higher juice content and higher sugar levels. In contrast, even if lower-quality cane has a similar juice content, it tends to have reduced sugar levels, especially if harvested prematurely.[79] The current study demonstrated that sugarcane can yield a substantial amount of juice, with an extraction of 74.6 ± 0.8%.

3.7. Optimization of sugarcane juice clarification using NAC

Optimizing pretreatment conditions is a critical step in developing an effective, cost-efficient pretreatment method. A key objective of this optimization was to identify the precise process parameters that maximize processing benefits, such as clarification efficiency, while also assessing their relative importance. Traditional methods that analyze one factor at a time are time-consuming and overlook potential interactions between multiple factors. In contrast, response surface methodology-central composite design (RSM-CCD) provides a more effective optimization strategy by evaluating several factors and their interactions simultaneously.

In this study, 21 experimental settings, including 2 central replicates and 23 total runs in Table 7, were used to optimize cane juice clarification. The process variables optimized were temperature, pH, clarification dosage, agitation speed, and time, and the responses were analyzed using Design-Expert software (v.13.0.5.0, USA). The data were fit to multiple regression quadratic polynomial models, setting the temperature, pH, time, agitation speed, and clarification amount to "in range". For turbidity and MV, the system responses were set to "minimized", while the conditions for color removal efficiency and settling rate were set to "maximized".

Several parameters were optimized to determine the optimal conditions for maximizing cane juice clarification efficiency. The effects of NAC dose (0.002–0.02%), pH (4–8), contact time (20–100 minutes), heating temperature (40 to 90 °C), and agitation speed (100 to 250 rpm) on clarification responses were studied. The experimental data were analyzed using RSM-CCD, facilitated by Design-Expert software (v.13.0.5.0, USA).

The experimental design and associated responses are summarized in Table 7, which demonstrates significant variability in the outcomes. Regression analysis of the independent and dependent variables was conducted using the methodology described in an earlier study.[46] Results indicated significant relationships ($p \leq 0.05$), as shown in Tables S5 and S6. Among the linear terms, pH emerged as the most significant factor, positively influencing the response with a coefficient of 523.10 and the highest *F*-value of 24 019.27. Lower pH levels within the studied range were more effective at reducing turbidity.

The NAC dose also showed a significant negative effect (−774.61), indicating that lower NAC doses led to increased turbidity, suggesting the need for higher NAC doses for effective clarification. A moderate NAC dose is essential for optimal results. Additionally, interactions among pH and temperature (*BD*), temperature alone (*D*), and time (*C*) demonstrated significant negative impacts on turbidity removal, with coefficients of −507.4, −384.92, and −528.66, respectively, highlighting their critical roles in the clarification process of sugarcane juice using NAC.

Among all the process parameters, factor *A* (NAC dose) emerged as the most influential across all response cases, as indicated in Tables S5 and S6. This was followed in significance by factors *B* (pH), *C* (time), and *D* (temperature). Notably, factor *E* (agitation speed) did not rank among the top five influential factors, suggesting it has the least impact on the outcomes. The *F*-value further supports this for factor *E*, which is lower than those of the other factors in Tables S5 and S6.

The analysis of variance (ANOVA) conducted on the juice clarification process parameters, detailed in Tables S5 and S6, revealed that the *p*-values for all regressions were less than 0.0001. This indicates that the model is statistically significant at a 99% confidence level and provides insights into the interaction patterns.[80,81] The respective higher *F*-values for the model were 7660.89, 37 614.13, 5062.25, and 10 842.68 for turbidity, settling rate, mud volume, and color removal efficiency, respectively, confirming the model's significance. Generally, a low "*p*" value for Fisher's statistic indicates a high level of significance for the regression model.

The lack-of-fit *F*-values, presented in Tables S5 and S6, were 1.29, 0.2232, 0.0457, and 1.59, with corresponding lack-of-fit *p*-values of 0.3122, 0.6388, 0.8317, and 0.2141 for turbidity, settling rate, mud volume, and color removal efficiencies, respectively. These non-significant results indicate that the model fits well. Additionally, the model exhibited low pure error, reflecting the high precision of the experimental results, as evidenced by the residual errors that accounted for the variation in responses.

The significance of the determination coefficient for the process parameters was further validated using the Student's *t*-test. A higher *t*-value and a smaller *p*-value suggest greater significance in the coefficient terms. The results from the Student's *t*-test and *p*-values demonstrate that most linear, quadratic, and interaction terms were highly or moderately significant, as shown in Tables S5 and S6, with *p*-values below 0.05. However, the interaction terms AB and C^2 in mud volume displayed *p*-values of 0.1299 and 0.3590, respectively, indicating non-significance. In terms of colour removal efficiency, the terms CE (*p*-value: 0.3506) and AC (*p*-value: 0.9532) were also non-significant.

3.7.1. Data reliability analysis. The cane juice clarification using NAC derived from the mixed fruit peels (MFPs) was performed, and the reliability of the obtained data (under RSM) was analyzed for turbidity reduction and decolorization

Table 7 Experimental results on turbidity, settling rate, mud volume, and color removal efficiency were analyzed to investigate the effects of NAC dose, pH, time, temperature, and agitation speed[a]

	Independent variables					Dependent variables (responses)			
Run	*A*	*B*	*C*	*D*	*E*	Turbidity (NTU)	Settling rate (cm min^{-1})	Mud volume (mL)	Color removal efficiency (%)
1	0.020	8	20	90	100	1833.15 ± 0.11^{k}	0.14 ± 0.01^{ghi}	6.98 ± 0.02^{cde}	73.35 ± 0.31^{g}
2	0.027	6	60	65	200	1399.86 ± 0.12^{q}	0.36 ± 0.03^{c}	7.56 ± 0.06^{bc}	90.40 ± 0.24^{d}
3	0.011	9.6	60	65	200	2816.36 ± 0.60^{f}	0.04 ± 002^{lm}	5.51 ± 0.05^{fgh}	67.16 ± 0.21^{kl}
4	0.011	6	60	19	200	2733.06 ± 0.99^{h}	0.07 ± 01^{jkl}	5.81 ± 0.21^{fg}	70.72 ± 0.40^{h}
5	0.020	8	20	40	250	3033.03 ± 0.20^{d}	0.06 ± 0.01^{jkl}	5.83 ± 0.11^{fg}	76.54 ± 0.41^{f}
6	0.011	6	60	65	200	2133.12 ± 0.11^{i}	0.20 ± 0.02^{ef}	6.27 ± 0.21^{ef}	73.55 ± 0.22^{g}
7	0.011	6	60	65	200	2133.12 ± 0.11^{i}	0.21 ± 0.02^{ef}	6.27 ± 0.21^{ef}	73.55 ± 0.22^{g}
8	0.011	6	60	111	200	1316.54 ± 0.32^{r}	0.46 ± 0.01^{a}	7.57 ± 0.11^{bc}	92.22 ± 0.23^{b}
9	0.011	6	12.8	65	200	2932.39 ± 0.59^{e}	0.44 ± 0.01^{a}	5.21 ± 0.41^{gh}	69.25 ± 0.30^{i}
10	0.002	8	100	40	250	3166.35 ± 0.89^{a}	0.06 ± 0.02^{kl}	4.49 ± 0.49^{h}	63.88 ± 0.51^{m}
11	0.002	4	20	40	100	3133.05 ± 0.62^{b}	0.08 ± 0.03^{jk}	4.86 ± 0.81^{gh}	66.55 ± 0.52^{L}
12	0.005	6	60	65	200	2766.39 ± 0.87^{g}	0.01 ± 0.02^{m}	4.82 ± 0.62^{gh}	68.35 ± 0.40^{ij}
13	0.020	4	100	90	100	1299.87 ± 0.22^{s}	0.40 ± 0.02^{b}	7.83 ± 0.41^{bc}	93.27 ± 0.31^{a}
14	0.020	8	100	40	100	1833.15 ± 0.11^{k}	0.12 ± 0.01^{hi}	6.29 ± 0.31^{def}	77.65 ± 0.33^{e}
15	0.002	8	100	90	100	1766.49 ± 0.82^{l}	0.16 ± 0.02^{gh}	6.96 ± 0.22^{cde}	73.46 ± 0.41^{g}
16	0.002	4	100	90	175	1633.17 ± 0.13^{n}	0.17 ± 0.04^{fg}	7.31 ± 0.31^{bcd}	77.11 ± 0.11^{ef}
17	0.011	6	132.8	65	200	1566.44 ± 0.10^{o}	0.11 ± 0.03^{ij}	7.91 ± 0.11^{bc}	74.05 ± 0.39^{g}
18	0.011	6	60	65	250	1683.16 ± 0.7^{m}	0.14 ± 0.03^{ghi}	7.36 ± 0.17^{bc}	73.26 ± 0.22^{g}
19	0.011	6	60	65	175	1849.95 ± 0.43^{j}	0.07 ± 0.03^{jkl}	6.94 ± 0.32^{cde}	69.33 ± 0.37^{i}
20	0.020	4	20	90	250	1499.85 ± 0.89^{p}	0.32 ± 0.01^{d}	7.97 ± 0.27^{bc}	91.12 ± 0.17^{cd}
21	0.002	8	20	90	250	3099.84 ± 0.23^{c}	0.07 ± 0.07^{kl}	4.93 ± 0.32^{gh}	67.81 ± 0.21^{jk}
22	0.02	4	100	40	175	1233.18 ± 0.36^{t}	0.22 ± 0.02^{1e}	8.13 ± 0.29^{b}	91.54 ± 0.32^{bc}
23	0.011	2.4	60	65	100	932.91 ± 0.65^{u}	0.40 ± 0.03^{b}	9.31 ± 0.31^{a}	93.44 ± 0.34^{a}

[a] Triplicate experiments were performed for each run ($n = 3$); *A*: nano activated carbon; *B*: pH; *C*: time (minutes); *D*: temperature (°C); *E*: agitation speed (rpm); all values are means ± standard deviation; mean values (along the column) share different superscripts that are significantly different ($p < 0.05$).

efficiency through SD (standard deviation) and SEM (standard error of the mean) error bars of the presently studied data. In the turbidity context, cane juice varied widely (a reduction range of 3166 to 933 NTU), indicating a strong dependence on operating conditions. The lowest turbidity in Fig. 8 was obtained in run 23 (932 ± 0.65 NTU), followed by runs 22 and 13, demonstrating optimal NAC performance at moderate dosage and contact conditions. Runs with insufficient NAC dose or unfavorable operating variables (*e.g.*, runs 10, 11, 21) showed poor turbidity reduction (3000 NTU). The small SD and SEM error bars across all runs confirm excellent experimental reproducibility and process stability.

In the present study, the sharp turbidity reduction observed in optimized runs highlights the effectiveness of fruit-peel-derived NAC in destabilizing colloids and adsorbing suspended impurities *via* surface charge interactions and porous adsorption. Compared with high-turbidity control-like runs (minimal clarification effect), optimized NAC conditions achieved >65–70% turbidity reduction in Fig. 8, indicating a clear practical advantage. The low SEM values (0.5 NTU in most cases) indicate statistically reliable performance, supporting NAC as a robust clarifier for cane juice applications.

Similarly, removal efficiency upon NAC-assisted cane juice clarification ranged from 63.88 ± 0.51% to 93.44 ± 0.34% in Fig. 8, indicating strong sensitivity to operating conditions. The highest decolorization was achieved in run 23 (93.44%), closely followed by runs 13 (93.27%), 8 (92.22%), 22 (91.54%), and 20 (91.12%), demonstrating the excellent performance of NAC under optimized variable conditions. Studied results found to be narrow SD and SEM bars across all experiments confirm high analytical precision and reproducibility.

The high color removal efficiencies observed in optimized runs highlight the strong adsorptive affinity of fruit-peel-derived NAC for melanoids, phenolics, and colored colloids in cane juice. Enhanced decolorization correlated with improved settling rates and higher mud volumes, indicating effective floc formation and impurity capture. Experimental runs with lower color removal exhibit control-like behavior, underscoring the importance of appropriate NAC dosage and process conditions. The consistently low SEM values (0.35%) demonstrate statistically reliable performance, confirming that NAC provides a robust, reproducible, and efficient alternative to conventional clarifiers for cane juice decolorization.

3.7.2. Effect of interaction between process variables. This study investigates how various factors, such as agitation speed, pH, carbon dose, contact time, and temperature, influence the removal of non-sugars from sugarcane juice using the clarificant (NAC).[52] The clarifying effectiveness of the optimized NAC was assessed under controlled laboratory conditions for these variables using Response Surface Methodology with Central Composite Design (RSM-CCD) *via* Design-Expert software (v. 13.0.5.0, USA). Key characteristics of carbons that

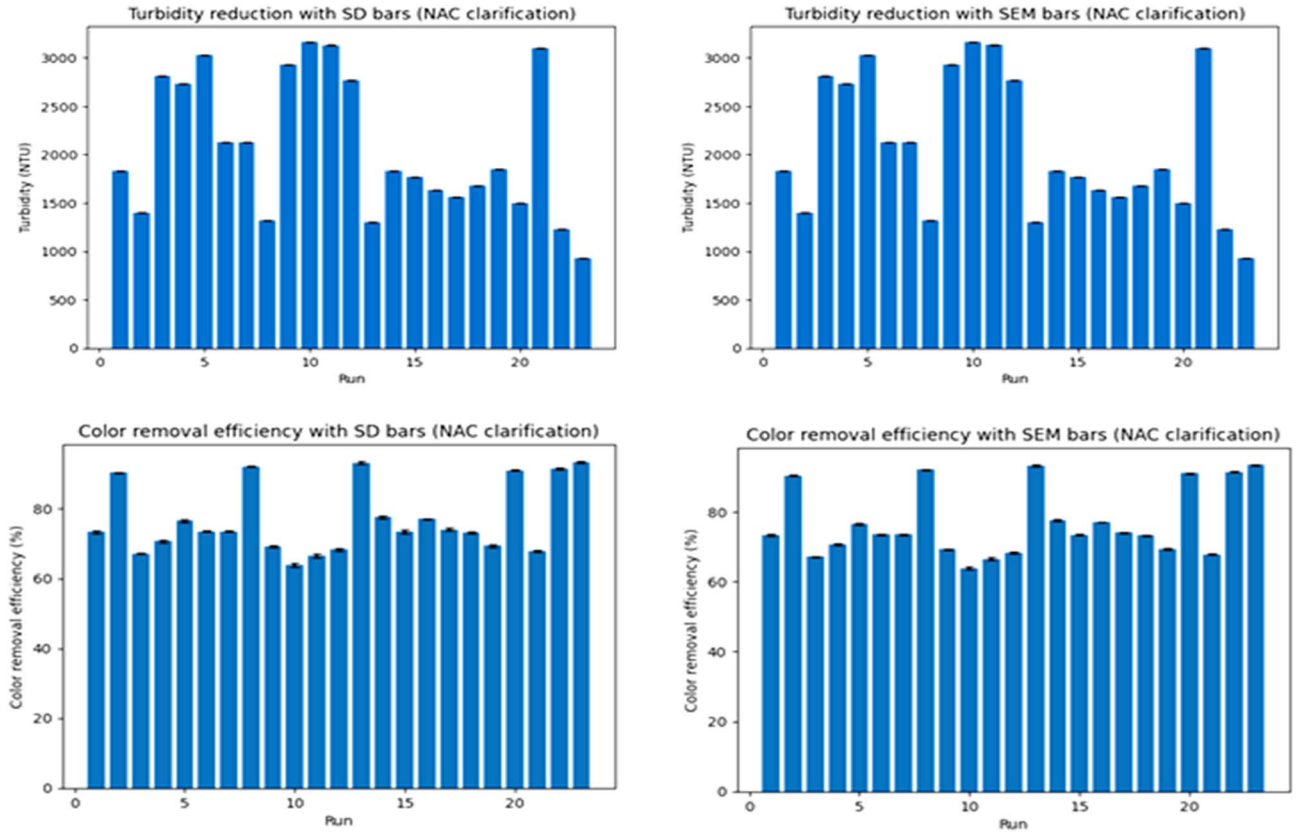

Fig. 8 Turbidity and decolorization efficiency (for SD and SEM error analysis) of NAC on cane juice clarification for the sulfur-free sugar production using RSM. Triplicate experiments were performed ($n = 3$).

impact clarification efficiency include total surface area, pore size distribution (relative proportions of micropores, mesopores, and macrospores), and chemical reactivity, which is determined by the types and concentrations of surface oxides present on the carbon surface.[52] Consequently, variations in the adsorbent properties led to differences in decolorization effectiveness. Additionally, pore size distribution and total surface charge contributed to the varying efficiencies of the adsorbents, which may not always correlate directly with the adsorbents' surface area.[57]

3.7.2.1. Effect of NAC dosage and pH on juice clarification. The impact of NAC dosage and pH on the clarification of sugarcane juice was examined by varying NAC concentration (0.002% to 0.02%) and pH (4 to 8), while keeping other experimental variables constant. Fig. 9a and b present the 3D response surface and contour plot, illustrating the interaction between NAC dosage and pH in the clarification process. The results indicate that increasing the NAC dosage from 0.002% to 0.02% increases the clarification efficiency. This improvement is likely due to the increased availability of adsorption sites and surface area provided by the higher NAC dosage, which facilitates greater adsorption of impurities (non-sugars) during cane juice clarification.

In some cases, the highest NAC surface area did not guarantee the maximum colour removal or turbidity reduction because cane juice clarification is controlled not only by surface area but also by pore accessibility, surface chemistry, and flocculation behaviour. A large fraction of the surface area in micropores is more effective for decolorization. In addition, surface function groups and charge interactions at pH 4 govern impurity adsorption and floc formation. Excessively high surface area can hinder particle bridging, producing poorly settleable flocs. Consequently, colour removal and turbidity reduction show a nonlinear relationship with BET surface area, with optimum performance achieved at balanced textural and surface properties rather than at maximum surface area.[21,23,56]

In the juice, both the surface charge of the NAC and the degree of ionization of certain impurities are influenced by pH. The pH level of the juice affects the adsorption of various ions, and the experiments were conducted within a pH range of 4 to 8. As depicted in Fig. 9a, the pH also plays a significant role in the clarification of cane juice.

The effectiveness of clarification, as shown in Fig. 9a, decreased as the solution pH increased from 4 to 8. This decline in efficiency may be attributed to increased surface attraction of the adsorbent or to an excess of H^+ ions, which promote charge interactions at the adsorption sites, thereby improving clarification in an acidic medium. Additionally, at lower pH levels, the reduction in negatively charged sites may strengthen electrostatic attraction, further enhancing clarification efficiency. Conversely, Fig. 9b indicates that turbidity was higher at lower NAC dosages and elevated pH, likely due to insufficient surface

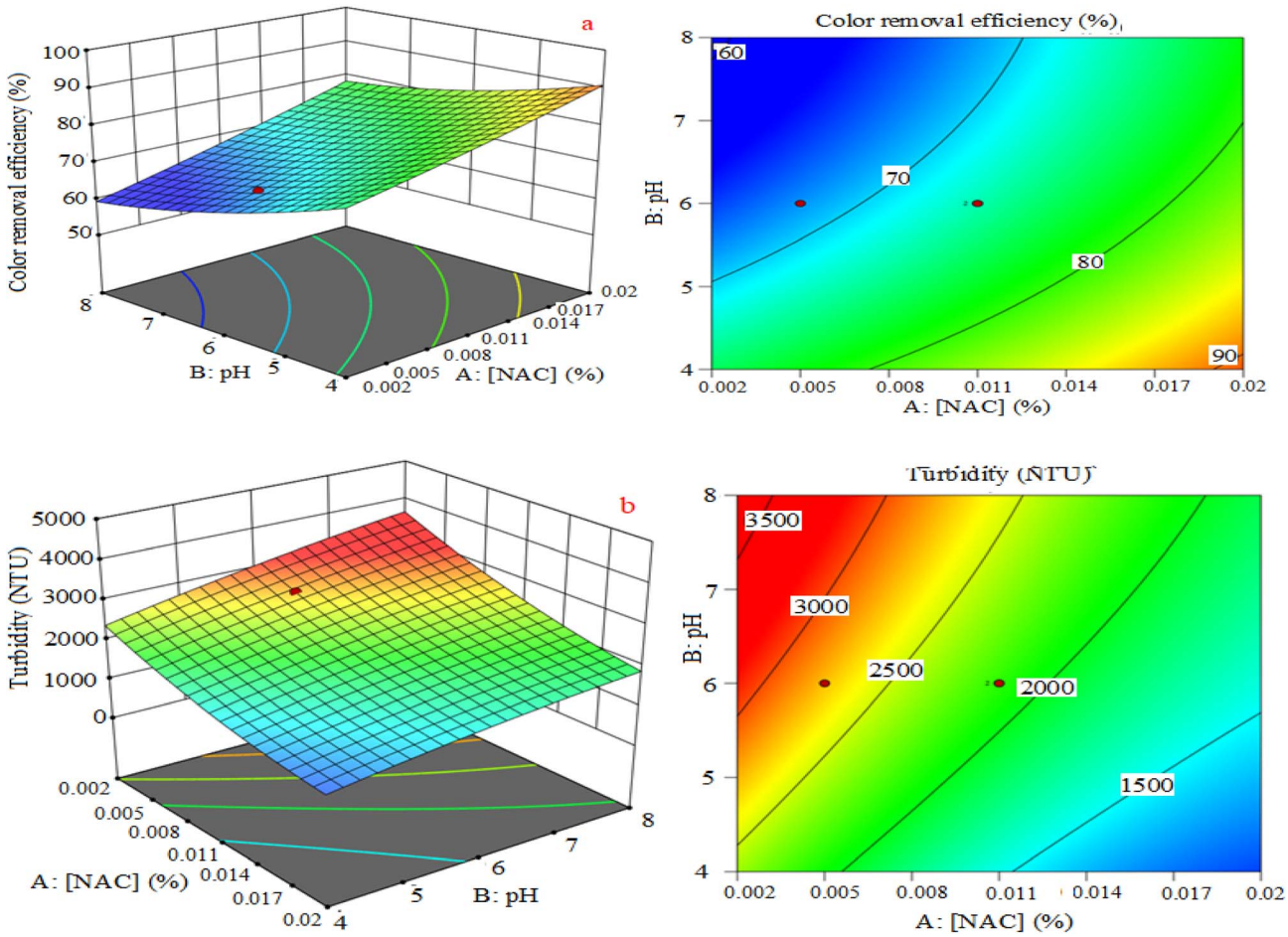

Fig. 9 The 3D surface and contour plot for the interaction effect of NAC dose and pH on color removal efficiency (a) and turbidity (b).

area at lower NAC concentrations and the greater influence of $^{-}$OH ions.

Also, the study highlights that, unlike conventional clarifiers such as lime or phosphoric acid, which primarily remove impurities *via* coagulation and precipitation by forming insoluble salts, NAC derived from fruit peels primarily functions through adsorption onto its high surface area (600 $m^2 g^{-1}$) and mesoporous structure. This allows selective capture of melanoidins, phenolics, and colloidal particles *via* hydrogen bonding, π–π interactions, and electrostatic attraction, rather than bulk chemical reactions. While minor flocculation may assist settling, adsorption dominates, enabling lower sludge volumes and residues, demonstrating a novel, sustainable alternative for cane juice treatment.[23,56]

3.7.2.2. Effect of NAC dosage and contact time on cane juice clarification. Fig. 10a shows that clarification efficiency increases to over 90% with higher NAC dosage and extended time, up to 60 min. This improvement suggests that a greater NAC dosage provides a larger surface area, enhancing the availability of adsorption sites for impurities. A similar pattern has been reported in the literature regarding the removal efficiency as a function of adsorbent dosage when using activated carbon derived from tea waste.[81,82]

In general, the duration of juice retention in the clarifiers significantly impacts both the juice and its components. Juice with a high concentration of suspended matter requires a longer retention time in the clarifier. This time can vary based on the clarification method used, as different methods may result in slower settling or longer reaction times for the defecant. For the Rapi-Dorr 444 clarifier, the recommended minimum retention time is 2 h, with a maximum of 3 h[83]

In the current study, clarification efficiency exceeds 90% with increasing contact time, as illustrated in Fig. 10a, and then reaches a saturation point. However, beyond this optimal threshold, a slight decrease in clarification efficiency was observed. This decline may be attributed to the saturation of available sites and the reduced impurities present in the cane juice. Additionally, the experimental results demonstrate that the clarification efficiency of NAC rises significantly during the initial phase of clarification, followed by a gradual increase with extended contact time. Eventually, this increase slows down as equilibrium is approached. This behavior suggests that a substantial number of vacant surface areas are initially available for adsorption. As the adsorption contact time increases, these surfaces become occupied, leaving fewer available sites. Consequently, the remaining surface area

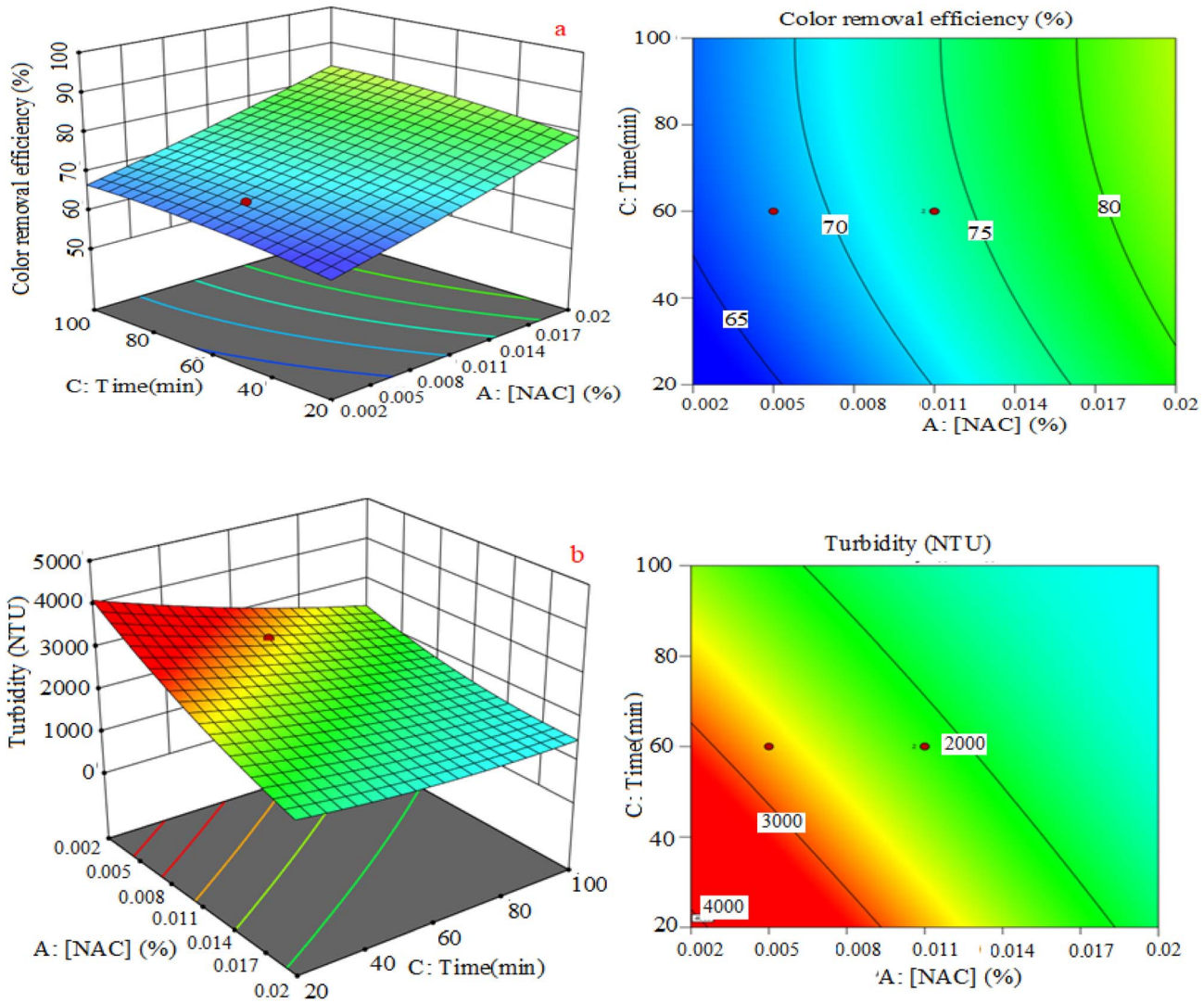

Fig. 10 The 3D surface and contour plot for the interaction effect of NAC dose and time on color removal efficiency (a) and turbidity (b).

becomes less effective at retaining impurities, slowing the process due to repulsive forces between the solute molecules and the adsorbent.

3.7.2.3. Effect of NAC dosage and heating temperature on cane juice clarification. The clarification of sugarcane juice is influenced by both NAC and temperature. In a study using 100 mL of sugarcane juice, the effects of temperature ranging from 40 to 100 °C and NAC concentrations from 0.002% to 0.2% on juice clarification were examined in Fig. 11. As depicted in Fig. 11, the efficiency of clarification with NAC improves as the temperature increases. This enhancement may be attributed to the reduced viscosity of the cane juice at higher temperatures.

Elevated temperatures facilitate a greater diffusion rate of adsorbate molecules through the external boundary layer and into the internal pores of the adsorbent particles. As the temperature rises, the kinetic energy of the sugarcane juice increases, thereby enhancing NAC's effectiveness in the clarification process. The temperature rise not only increases the number of active sites available on the NAC but also alters the clarifying agent's ability to reach equilibrium with impurities present. The endothermic nature of this reaction is evident as well. Furthermore, the interaction between the clarifying agent and contaminants may create new active sites. At the same time, the accelerated intraparticle diffusion of clarifying molecules into the NAC pores contributes to the overall improvement in clarification capacity.

3.7.2.4. Effect of NAC dosage and agitation speed on clarification of cane juice. Using an initial juice volume of 100 mL, the effects of NAC dosage and agitation speed were examined by varying NAC concentration from 0.002% to 0.02% and agitation speed from 100 to 250 rpm. The interaction between NAC dosage and agitation speed on the clarification of sugarcane juice is illustrated in a 3D contour plot, as presented in Fig. 12.

This plot indicates that higher agitation speeds facilitate the time required for the adsorbate to achieve the desired equilibrium. However, prolonged agitation reduces clarity by occupying active sites on the adsorbent. Notably, an agitation speed of around 100 rpm was found to positively influence clarity.

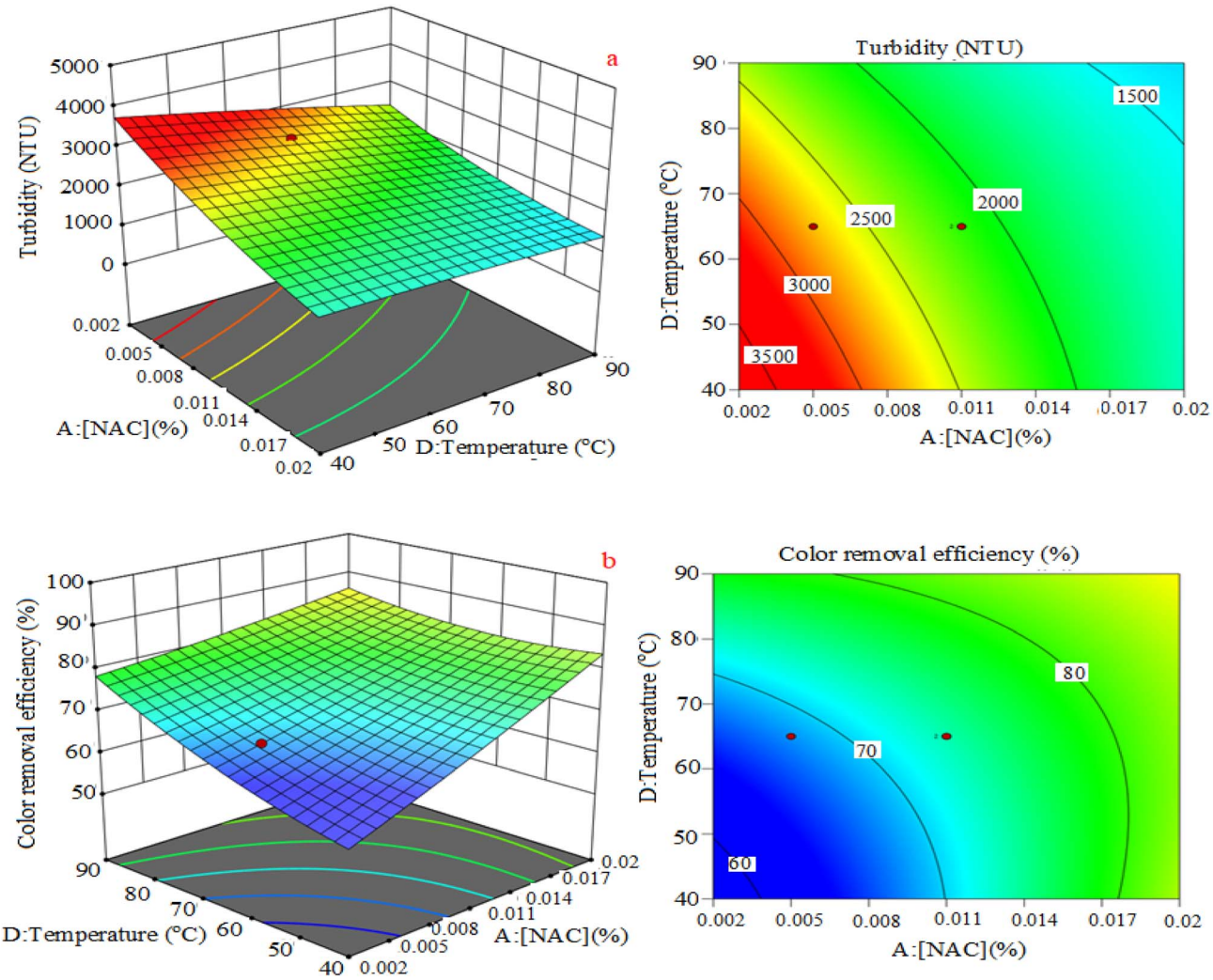

Fig. 11 The 3D surface and contour plot for the interaction effect of NAC dose and temperature on turbidity (a) and color removal efficiency (b).

Conversely, as agitation speed increased further, the clarification process's effectiveness diminished, likely due to increased interactions between the contaminants and the adsorbent surface.

3.7.3. Validation of optimum conditions for clarification of sugarcane juice using NAC. The statistical optimization of the clarification process typically aims to achieve desired outcomes across various responses and influencing factors.[84] In this case study, numerical optimization was used to enhance settling rates and colour removal efficiencies while reducing turbidity and mud volume, all within specified factor ranges. Fig. 13 illustrates the maximum desirability for optimal conditions based on the levels of NAC dose (0.002–0.02%), pH (4–8), contact time (20–100 min), heating temperature (40–90 °C), and agitation speed (100–250 rpm), resulting in the highest clarification efficiency. The optimal conditions yielded maximum responses of 1760.64 NTU for turbidity, a settling rate of 0.93 cm minute^{-1}, a mud volume of 6.7 mL/100 mL, and a color removal efficiency of 97.4%. These results were achieved at an NAC dose of 0.0105%, pH 4, contact time 20 min, heating temperature 90 °C, and agitation speed 100 rpm.

In the current study, the operating pH of 4 was found to clarify cane juice using NAC, whereas pHpzc was 2.0 in Fig. 3, indicating that the adsorbent surface becomes negatively charged at pH 4, favoring electrostatic attraction with cationic pollutants while repelling anions. Optimal clarification at pH 4 is described by a synergistic mechanism: π–π (n–π) interactions between aromatic domains and adsorbates, and hydrogen between surface –OH/–COOH groups and polar molecules. Thus, adsorption efficiency arises from a combination of electrostatic attraction and non-electrostatic forces, ensuring effective contaminant removal under mildly acidic conditions.[85,86] The suitable adsorption mechanism, as shown in this study in Fig. 14.

3.8. Physicochemical characteristics of raw cane juice, clarified juice, and produced raw sugar

Essential quality assessments are crucial, as they can reveal distinct patterns and characteristics of sugar, including purity

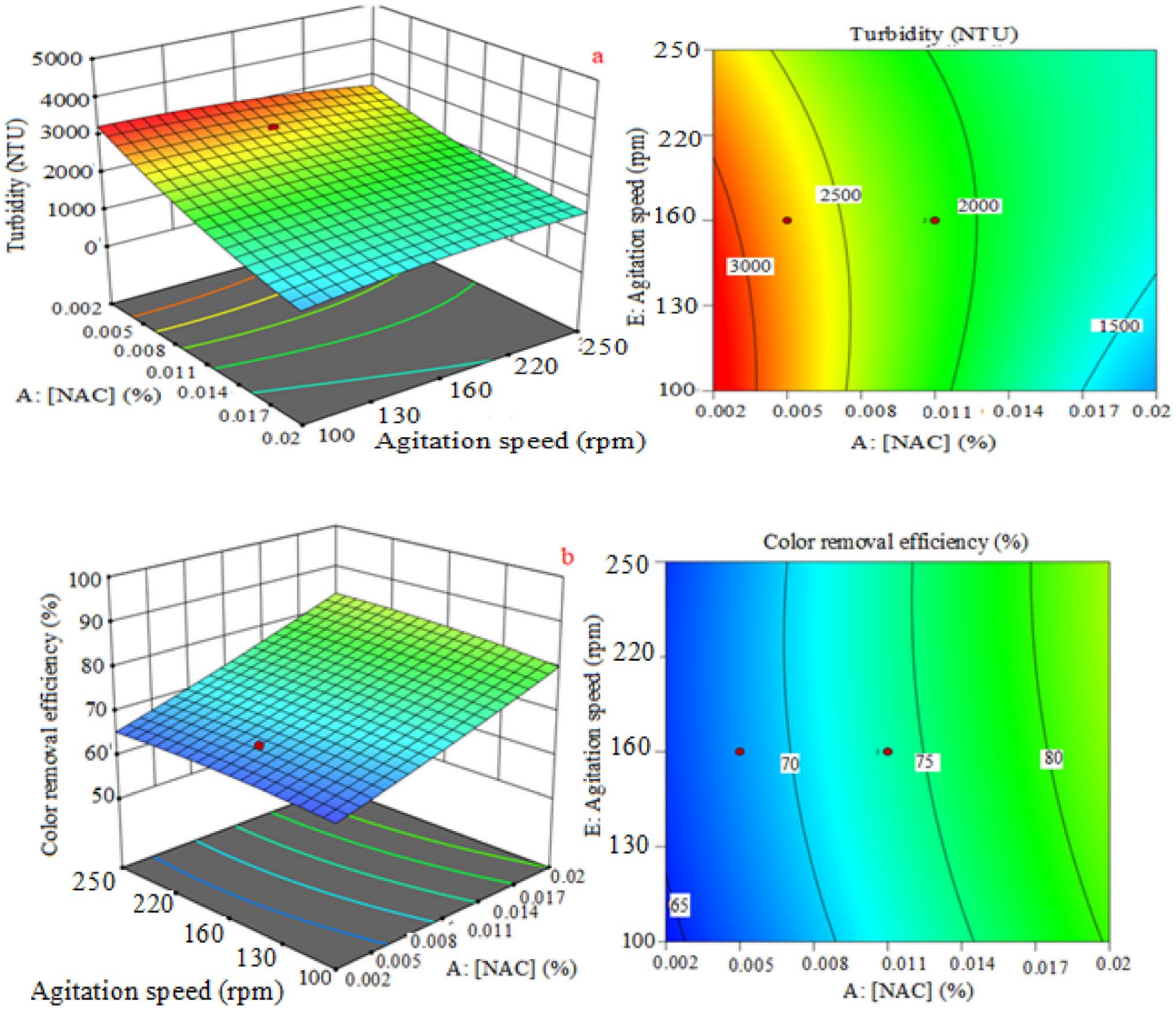

Fig. 12 The 3D surface and contour plot for the interaction effect of NAC dose and Agitation speed on turbidity (a) and color removal efficiency (b).

(measured by polarization), color, humidity, and the presence of insoluble contaminants (impurities and insoluble solids). The key parameters evaluated included moisture content, ash content, Brix, Pol%, pH, reducing sugars, color, turbidity, settling rate, and mud volume for raw sugarcane juice, treated/clarified juice, and the final produced sugar. The results of these assessments are detailed in Table 8.

3.8.1. Yield of juices and produced raw sugar. The juice yields obtained from the extraction process, milling, and clarification of raw juice using NAC as a clarifier were reported as 74.6 ± 0.87% and 94.64 ± 0.05%, respectively in Table 8. This suggests that processed sugarcane yields more juice and produces less fibrous bagasse. Additionally, the processed juice contains lower levels of non-sucrose components (excluding water). The effectiveness of NAC as a clarifier is evident, as it resulted in a tenfold reduction in the turbidity of the clear juice and an increase in its yield, as shown in Table 8. The yield of raw sugar from the clarified juice was measured at 13.15 ± 0.48%, as shown in Table 8, which aligns closely with previous findings reporting a yield of 13.03%.[87] Therefore, the results of this study reinforce the notion that NAC is an effective clarifier for eliminating non-sucrose substances from cane juice in the sugar production process.

3.8.2. Boiling house recovery of sugar. Boiling house recovery (BHR) encompasses processes such as clarification, evaporation, crystallization, separation, and drying, similar to those used in sugar-finishing operations. Typically, BHR values exceed 80%, indicating that the processing methods applied to sugarcane juice are commendable.[88] In this study, the reported BHR is 85.88 ± 1.05%, demonstrating the efficient recovery of sucrose from the processed clear juice. This suggests that clarified cane juice, along with NAC and other finishing processes (such as evaporation, crystallization, separation, and drying), has been effectively used in sugar production.

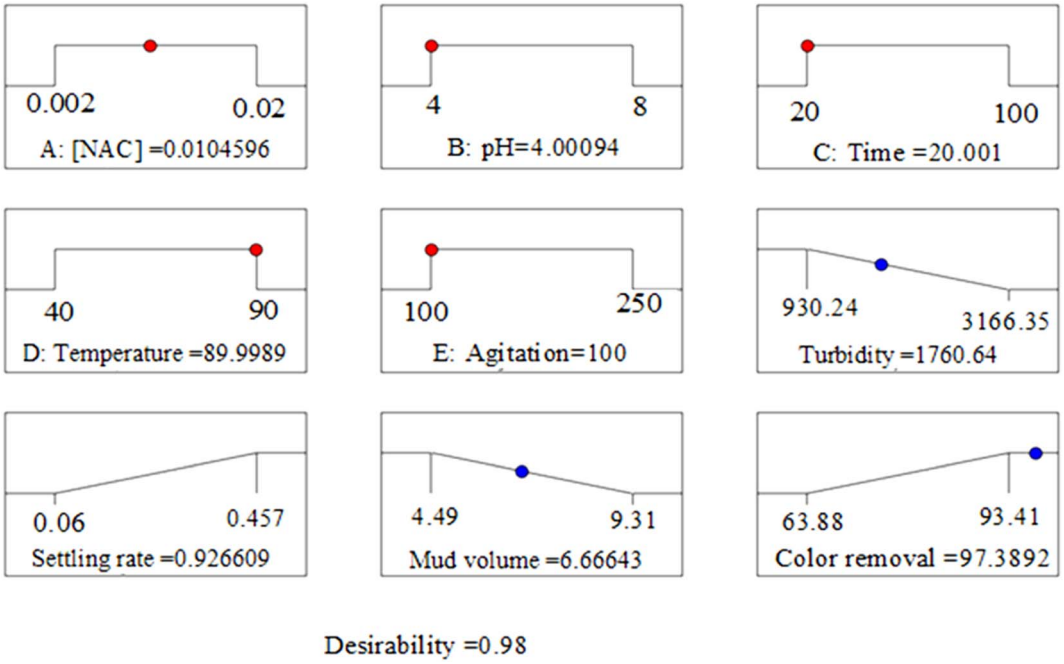

Fig. 13 Ramp desirability plots for the optimization of factors and responses for cane juice clarification using NAC under RSM.

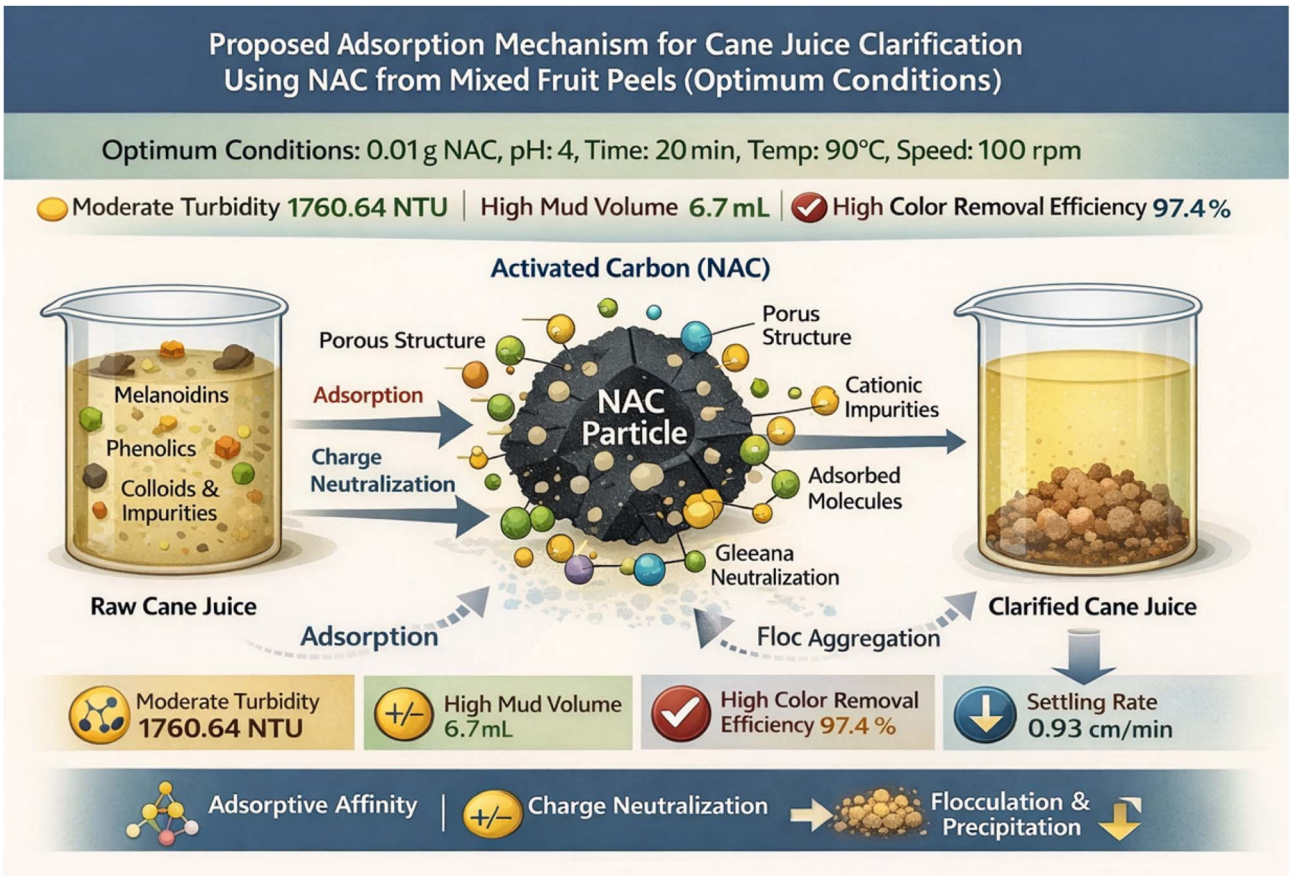

Fig. 14 Proposed adsorption mechanism of avocado-banana-papaya mixed peels-derived NAC on cane juice clarification at optimized conditions by RSM.

Table 8 Physicochemical characterization of raw, clarified cane juice by NAC and produced sugar[a]

Studied parameters	Raw juice (untreated)	Treated (clear) juice	Produced sugar
Yield (%)	74.6 ± 0.87	94.64 ± 0.05	13.15 ± 0.48
BHR (%)	—	—	85.88 ± 1.05%
pH	5.4 ± 0.02	4.00 ± 0.01	6.99 ± 0.07
Pol	15.8 ± 0.05	15.4 ± 0.02	13.57 ± 0.09
Brix	19.03 ± 0.05	17.02 ± 0.17	14.12 ± 0.12
Purity (%)	83.1 ± 0.49	90.4 ± 0.39	96.18 ± 0.24
Reducing sugar (%)	0.46 ± 0.01	0.48 ± 0.03	0.38 ± 0.02
Turbidity (NTU)	16 260.5 ± 0.5	1285.78 ± 0.25	—
Color (IU)	9623.54 ± 0.24	470.16 ± 0.05	422.85 ± 0.15
Settling rate (cm min^{-1})	0.59 ± 0.01	—	—
Mud volume (mL/100 mL)	5.5 ± 0.03	—	—
Moisture contents (%)	—	—	0.89 ± 0.03
Ash contents (%)	—	—	0.62 ± 0.01

[a] Data expressed as means ± standard deviation of triplicate experiments ($n = 3$).

3.8.3. The pH of the juice and the produced sugar. In this study, the pH values of the raw juice, treated juice, and produced sugar were measured at 5.4 ± 0.02, 4.00 ± 0.01, and 6.99 ± 0.07, respectively. According to the Ethiopian Sugar Corporation's standards, the recommended pH range for raw and clarified juice is 5.0–5.6. The raw juice's pH of 5.4 ± 0.02 indicates it is slightly acidic, consistent with previous findings.[89] This suggests that the raw juice likely contains water, sucrose, and various soluble and insoluble substances. After clarification with NAC, the pH of the clarified juice was 4.00 ± 0.05, indicating it is more acidic than the raw juice. The pH of the produced sugar was neutral, at 6.99 ± 0.07, consistent with the reported results.[90] The guidelines in the EAS EDICT (2010) should be taken into account during the clarification process for sugar production. Specifically, maintaining the clarified juice and syrup at pH 7.0 is crucial to prevent sucrose degradation due to acidity or alkalinity and to achieve sugar crystals with a pH range of 6.9 to 7.02.[52] In contrast, this study treated the juice at pH 4, which resulted in neutral sugars, likely because the sucrose lacked acid.

3.8.4. Turbidity. Turbidity and color have a greater influence on the efficiency of juice clarification than other factors. The main goal was to reduce turbidity, as monitoring it provides a reliable measure of clarifying effectiveness.[91] The turbidity in sugarcane juice arises from suspended particles and natural organic matter (NOM).[92] These negatively charged particles repel each other, preventing aggregation and settling while also transporting unwanted microbes and pollutants. To optimize sugar yield, it was essential to maximize non-sugar removal, eliminate suspended and colloidal impurities, remove colorants, and achieve a brilliant, light-colored, transparent juice free of suspended particles. Additionally, efforts were made to minimize sucrose loss due to inversion into glucose and fructose, as well as to degradation into organic acids.[92]

In this study, the turbidity levels of the unclarified and treated juice were measured at 16 260.5 ± 0.5 NTU and 1285.78 ± 0.25 NTU, respectively. They reported that turbidity in treated juice ranged from 4669 to 11 534 NTU, depending on the amount of clarificant used.[4] The results of this investigation indicated that the clarificant for sugarcane juice treatments exceeded expectations. The initial turbidity of the raw juice was approximately 16 260.5 ± 0.5 NTU, but after clarification, it decreased to 1285.78 ± 0.25 NTU.

3.8.5. Reducing sugar. The analysis revealed that the reducing sugar (RS) composition of the raw juices, specifically glucose and fructose, was measured at 0.46 ± 0.01%. Previous studies have indicated that the RS content in juices from various cane types ranges from 0.20% to 0.6%.[93] The RS value obtained from this study aligns well with these reported figures, suggesting an optimal yield of the product. An investigation of cane juices found that their reducing sugar content varied from 0.3% to 3.0%.[94]

The raw juice in this study, containing 0.46 ± 0.01% RS (which includes glucose, fructose, *etc.*), complies with ICUMSA standards. Additionally, the reducing sugar content of the clarified juice (processed with NAC) was determined to be 0.48 ± 0.03%. There was no significant difference between the raw and clarified juices, as both met the national standard for reducing sugar content, which limits it to 0.5%. The sugar produced in this study exhibited a reducing sugar content of 0.38 ± 0.02%.

A higher RS level suggests that the selected raw material may not have been fully matured. Furthermore, inadequate control of processing temperatures can degrade monosaccharides, leading to color that may worsen during storage.[95] This indicates that, in this study, the sugarcane was fully mature and that processing temperatures were maintained at optimal levels, minimizing saccharide breakdown and resulting in high-quality sugar production. The ideal RS concentration for white sugar should be between 0.20% and 0.65%.[93] The RS values of the sugar samples analyzed in this study fall within the recommended range.,[93] suggesting that the NAC clarification method could be a promising clarifying agent for sugar production.

3.8.6. Brix and pol of the juice. Pol%, which indicates higher product quality, also measures the ability to sweeten other substances.[96] Unlike Brix values, which reflect the total dissolved solids in 100 g of juice, pol provides insight into the sucrose content specifically. In this study, the Brix and pol of

raw cane juice were 19.03 ± 0.05% and 15.8 ± 0.05%, respectively, while the clarified juice had Brix values of 17.02 ± 0.17% and pol of 15.4 ± 0.1%. These figures represent the total solids and total sucrose content. They fall within the ranges reported.,[97] who noted brix values between 15.26 ± 0.45% and 21.89 ± 3.2%, and pol values between 13.11 ± 0.42% and 18.35 ± 0.03%. Consequently, the findings of this study align with the existing literature, confirming that the raw juice sample contains a significant amount of sugar, which is essential for further processing and production.

Pol represents the apparent sucrose content of a substance, expressed as a percentage by mass and determined using the single or direct polarization method. One advantage of employing NAC to clarify sugarcane juice is its dual benefit of enhancing juice clarity (purity) and Brix, as the pol% reflects both the quantity and purity of sucrose in the juice. The pol and brix values of the sugar currently produced were measured at 13.57 ± 0.09 and 14.12 ± 0.12, respectively. Several variables significantly influence the importance of sugar polarization.[98] Variability in processing conditions and the presence of coloring agents may contribute to the lower pol values observed, suggesting that impurities could impact this measurement. Higher pol values might indicate a greater quantity of sugar present.

3.8.7. Moisture content. The moisture content in sugar is linked to the honey/molasses film that remains on the crystals, which is not effectively removed during centrifugation due to inadequate centrifugation techniques.[99] When examining the processing of CTC4 and CTC14 sugarcane, it was found that the addition of clarificant to the juice treatments significantly affected the moisture content of the resulting sugar, leading to a reduction in water trapped within the sugar crystals.[98] The moisture level observed in the sugar studied was 0.89 ± 0.03, which is higher than the 0.5% moisture reported,[100] for VHP sugars produced from two different types of sugarcane.

3.8.8. Color of juice. Juice production necessitates an effective clarification system; a clarifying agent can eliminate coloring compounds that meet the standard color requirements for cane juice, as outlined in ref. 95. The raw sugarcane juice analyzed in this study exhibited the highest color values (9623.54 ± 0.24 IU), indicating the presence of numerous color-forming agents, including phenolic compounds, which contribute to the juice's vibrant appearance. The untreated juice has a color range of 15 957–12712 IU, which necessitates processes such as sulphation, defecation, and carbonation for clarification.[101] The color of the juice can vary depending on the chosen clarifier, as noted.[4] Consequently, a method is required to render the sugar produced in this study more palatable and suitable for human consumption.

The current color value is considered excessively high and must be reduced to ensure the production of high-quality sugar. However, the clarified juice color was significantly lowered to 470.78 ± 0.05 IU, demonstrating that NAC (Nano activated carbon) achieves optimal results in cane juice clarification. Given NAC's remarkable efficiency in removing color-causing substances from raw juice, it has the potential to serve as a viable alternative to chemical clarifiers commonly used in many sugar factories today. This shift to NAC could enhance the effectiveness of the clarification process, reduce reliance on imports, and promote the health of consumers of the produced sugar. The color values of the sugars synthesized in this study were measured at 422.85 ± 0.15 IU.

3.8.9. Settling rate. A crucial factor influencing settling rate is the Brix content of the raw juice. Research indicates that the brix percentage of raw juice should not exceed 16, as lower brix levels (total solids) are associated with improved settling rates. Consequently, it is essential to maintain the juice brix below 16 to achieve an optimal settling rate. Additionally, an increase in NAC concentration further enhances the settling rate. For the raw juice in this study, the settling rate recorded was 0.59 ± 0.01 cm minute^{-1}, as detailed in Table 8.

3.8.10. Mud volume. In the present study, optimal conditions yielded a mud volume of 5.5 ± 0.03 mL/100 mL. Mud volume (MV) measurements are used to assess the clarity of cane juice.[97] Consequently, when comparing the clarifying efficiency of the current study's MV with that reported in the existing literature,[102] the NAC reduced the juice's mud volume to 5.5 ± 0.03, as illustrated in Table 8.

3.8.11. Purity. The purity of a sugar product is determined by the ratio of sucrose content (pol) to total soluble solids (brix). The purity of untreated and clarified juices is 82.1% and 88.5%, respectively.[103] These findings align closely with the results in Table 8 of this study, which indicate that the purity of raw and treated juice is 83.10 ± 0.49% and 90.40 ± 0.3%, respectively. Both the raw and clarified juices meet the minimum purity requirement of 8% as per ESC standards, and were found to be within the upper limits set by national standards for this investigation.

The purity of sugar is influenced by processing methods, the number of chemical additives used in cane juice, and the variety of sugarcane employed.[104] For instance, Demerara sugar in Brazil has purity values ranging from 93.09% to 98.88%, crystal sugar purity ranges from 98.87% to 100.00%, and refined sugar values span from 93.39% to 99.70%.[103] The current study determined the sugar's purity to be 96.18 ± 0.24%, categorizing it as high quality according to the ICUMSA standard.[95] This high purity indicates that sulphited sugar is considerably better refined. However, the application of technology can yield sugar products with varying levels of color and turbidity.[79] Therefore, the sugar produced in this study still requires additional processing steps to enhance its palatability and make it suitable for human consumption.

3.8.12. Ash content. Ash concentration is a key indicator of sugar quality, influencing both purity and the presence of insoluble residues, which can cause sugar to darken during processing. A high ash concentration often indicates elevated levels of potassium and other minerals, which can inhibit sucrose crystallization in sugarcane juice and lead to undesirable sensory attributes, such as off-flavors.[105]

The sugar currently produced has an ash content of 0.62 ± 0.01% (see Table 8), which falls well within the Codex maximum limit of 3.5%.[2] These findings align with the values reported.[106] Additionally, the ash consumption limit set by standards in India, East Africa, and Ethiopia is 0.76%, indicating that our

results are nearly within this recommended range. Consequently, the produced sugar is largely compliant with the standards of various countries and is likely to be considered acceptable. Moreover, the use of natural NAC clarificant enhances the quality of the sugar, keeping it within the recommended ash limits.

3.9. Regenerative, cost, and scalability of NAC from fruit peels

Nano activated carbon derived from fruit peel waste offers a highly attractive economic profile for industrial cane juice clarification, thanks to its low-cost, abundant feedstock and minimal reliance on harmful chemicals during preparation. Agro-waste fruit peels, such as banana, papaya, and avocado, are locally available, often considered disposal liabilities, and can be used to produce NAC, making it both cost effective and environmentally beneficial.[23] Preliminary cost analyses indicate that NAC can be produced at a fraction of the cost of commercial powdered activated carbon (PAC) or granular activated carbon (GAC), particularly when utilizing simple chemical activation (*e.g.*, phosphoric acid) and low-energy carbonization.[56]

From a regenerative perspective, NAC demonstrates promising stability, with multiple adsorption–desorption cycles showing minimal loss in color removal efficiency or turbidity reduction, suggesting that the material can be recycled several times, reducing operational costs and waste generation. The process is scalable, as carbonization and activation units can be integrated into agro-industrial setups with continuous feedstock supply, supporting large-scale applications. Moreover, NAC's robustness under variable pH, temperature, and turbidity conditions further enhances its industrial applicability. Collectively, the combination of low feedstock cost, ease of preparation, regenerability, and scalability positions NAC as a practical, sustainable alternative to conventional clarifiers, potentially reducing both economic and environmental burdens of cane juice clarification.[23,107]

4. Conclusions

The preparation of nano activated carbon (NAC) involved activating H_3PO_4, followed by carbonization and subsequent reduction to the nanoscale. Using Response Surface Methodology – Central Composite Design (RSM–CCD), optimal synthesis conditions were determined: an impregnation ratio of 1 : 1.6 (sample-to-acid), a carbonization temperature of 410 °C, and a carbonization duration of 100 min. Characterization of the samples was conducted using FTIR, XRD, and SEM. Results from XRD and SEM indicated that the NAC particles exhibited an average size of 24.46 nm and a surface area of 650.87 ± 0.26 $m^2\ g^{-1}$.

In sugar production, clarifying sugarcane juice is a crucial step. Using a clarifying agent made from MFP presents a practical, cost effective solution for this process. This study investigated the use of NAC synthesized from MFP under optimal conditions as a clarifying agent for sugarcane juice. The established optimal conditions for clarification included a NAC concentration of 0.01%, a pH of 4, a clarification time of 20 min, a temperature of 90 °C, and an agitation speed of 100 rpm. The application of MFP-NAC resulted in a turbidity of 1760.6 NTU, a settling rate of 0.9 mL min^{-1}, a mud volume of 6.6 mL/100 mL, and a color removal efficiency of 97.4%.

Additionally, the clarified juice was processed into raw sugar, and its physicochemical properties were analyzed and found to comply with ICUMSA and Ethiopian sugar standards, demonstrating favorable outcomes. Thus, this study concludes that the low-temperature phosphoric acid-treated nanoactivated carbon is a promising adsorbent for the removal of pigments, dyes, inorganic substances, and organic impurities from aqueous solutions, as well as for reducing CO gas emissions. Furthermore, the results support the potential of MFP-NAC as an effective clarifying agent for sugarcane juice in sugar production.

Author contributions

Conceptualization, data curation, methodology, software, validation, and writing – original draft, W. R. B; supervision, conceptualization, data curation, validation, software, and writing – review and editing, G. M. F., R. D. All authors have read and agreed to the published version of the manuscript.

Conflicts of interest

The authors declare that there is no conflicts of interest regarding the publication of this paper.

Data availability

The supporting data has been provided as part of the supplementary information (SI). Supplementary information: Table S1: experimental design for optimizing the fruit peel powder mixing proportion and the nano activated carbon preparation; Table S2: experimental design for the clarification of cane juice for raw sugar production; Table S3: ANOVA results for the quadratic model of percent carbon yield obtained from the mixed fruit peels (MFP) under carbonization; Table S4: analysis of variance (ANOVA) results for the fixed carbon contents and surface area on synthesized nano activated carbon (NAC) from mixed fruit peel wastes; Table S5: results of analysis of variance for the turbidity and settling rate in clarification of cane juice using NAC; Table S6: results of analysis of variance for the mud volume and color removal efficiencies in clarification of cane juice using NAC. See DOI: https://doi.org/10.1039/d6ra01408a.

Acknowledgements

The authors thank the College of Natural and Computational Sciences, Arba Minch University, Department of Chemistry, for access to the laboratory facilities. Also, thank you to the Department of Materials Science and Engineering at Adama Science and Technology University for the sample characterization techniques using FTIR, XRD, and SEM.

References

1 G. Eggleston, Hot and cold lime clarification in raw sugar manufacture II. Lime addition and settling behavior, *Int. J. Sugar Technol.*, 2000, **102**(1221), 453–457.
2 P. Patricia and R. H. Moretti, Study of clarification process of sugar cane juice for consumption. Ciênc. eTecnolgia de Alimentos, Campinas, *Food Sci. Technol.*, 2010, **30**, 776–783.
3 W. O. S. Doherty, Improved sugar cane juice clarification by understanding calcium oxide-phosphate-sucrose systems, *J. Agric. Food Chem*, 2011, **59**, 1829–1836.
4 T. Birhanu, M. M. Makur and R. Duraisamy, Evaluation of Okra (Abelmoschus esculentus) Powder and Nano CaO as Alternative Clarifiers for Lime in the Processing of Sugarcane Juice, *Sugar Tech*, 2024, **26**, 446–468.
5 A. Mani, S. Palanivel, S. Palanivel and Th. Palvannan, Optimization of orange-G dye adsorption by activated carbon of *Thespesia populnea* pods using response surface methodology, *J. Haz. Mate*, 2011, **186**, 827–834.
6 M. T. Amin, A. A. Umair and U. Manzoor, A review of removal of pollutants from water/wastewater using different types of nanomaterials, *Adv. Mate. Sci. Engg*, 2014, **1**, 1–24.
7 K. Vinod, I. T. Gupta, H. Sadeg, S. Behnam and M. Behnam, Nanoparticles as an adsorbent; A positive approach for removal of noxious metal ions: A review, *Sci. Technol. Develop*, 2015, **34**, 195–214.
8 Z. Jianming, Z. Shang-Ru, Li. Shi and Ge. Tian, Pb (II) removal of Fe_3O_4-SiO_2-NH_2 core-shell nanomaterials prepared via a controlled sol-gel process, *Chemi. Engg. J*, 2013, **215**, 461–471.
9 R. Cucun, S. Muhamad and M. A. Yohanes, Synthesis and characterization of nano activated carbon from annatto peels (*Bixaorellana L.*) viewed from temperature activation and impregnation ratio of H_3PO_4. EKSAKTA, *J. Sci. Data Anal*, 2020, **20**, 44–50.
10 J. L. Park, C. Ryu, K. S. Gang, W. Yang, Y. K. Park, J. Jung and S. Hyun, Comparison of biochar properties from biomass residues produced by slow pyrolysis at 500°C, Bioresource, *Technol*, 2013, **148**, 196–201.
11 Li. Koon-Yang, Q. Hui, H. T. Feng and B. Alexander, Bacterial cellulose is a source of activated nanosized carbon for electric double-layer capacitors, *J. Mate. Sci*, 2013, **48**, 367–376.
12 M. E. Fernandez, G. V. Nunell, P. R. Bonelli and A. L. Cukierman, Activated carbon developed from orange peels: batch and dynamic competitive adsorption of basic dyes, *Ind. Crops and Prod.*, 2014, **62**, 437–445.
13 P. Nowicki, J. Kazmierczak-Razna and R. Pietrzak, Physicochemical and adsorption properties of carbonaceous sorbents prepared by activation of tropical fruit skins with potassium carbonate, *Mate. & Design*, 2016, **90**, 579–585.
14 N. S. Razali, A. S. Abdulhammeed, A. H. Jawad, A. L. Othman, Z. A. Yosuf, T. A. Al-Duaij and O. K. N. S. Alsaiari, High-surface-area-activated carbon derived from mango peels and seeds wastes via microwave-induced $ZnCl_2$ activation for adsorption of methylene blue dye molecules: statistical optimization and mechanism, *Molecules*, 2022, **27**, 6947.
15 J. Darayen, W. Theerawong, N. Sriprach and C. Vukthong, Comparative study on acetic acid adsorption using activated carbon derived from banana and pineapple peels, *J. Info. Syst. Engg. Mangt*, 2022, **10**, 472–478.
16 R. K. Widi, P. Setyopratomo, P. E. Danatha, V. D. Nanlohy and E. Savitri, Preparation and characterization of activated carbon from Cavendish banana (*Musa acuminata*) peels for ferric ions adsorption, *Inter. J. Tech*, 2022, **16**, 1362–1374.
17 G. Yirdaw, A. Dessie and T. A. Birhan, Optimization of process variables to prepare activated carbon from Noug (*Guizotia abyssinica cass.*) stalk using response surface methodology, *Heliyon*, 2023, **9**, e17254.
18 N. Rambabu, B. V. Rao, V. R. Surisetty, U. Das and A. K. Dalai, Production, characterization, and evaluation of activated carbons from de-oiled canola meal for environmental applications, *Industrial Crops and Products*, 2015, **65**, 572–578.
19 A. K. Tolkou, K. N. Maroulas, D. Theologis, I. A. Katsoyiannis and G. Z. Kyzas, Comparison of Modified Peels: Natural Peels or Peels-Based Activated Carbons for the Removal of Several Pollutants Found in Wastewaters, *C.*, 2024, **10**, 22.
20 J. A. Solis-Fuentes, F. Galan-Mendez, M. D. R. Hernandez-Medel, R. S. Garcia-Gomez, M. Bernal-Gonzalez, S. Mendoza-Perez and M. D. C. Duran-Dominguez-de-Bazua, Effectiveness of bagasse activated carbon in raw cane juice clarification, *Food Bioscience*, 2019, **32**, 100437.
21 W. O. S. Doherty, C. M. Fellows, S. Gorjian, E. Senogles and W. H. Cheung, Flocculation and sedimentation of cane sugar juice particles with cationic homo- and copolymers, *J. Appl. Poly. Sci*, 2003, **90**, 316–325.
22 K. Salelign and R. Duraisamy, Sugar and ethanol production potential of sweet potato (*Ipomoea batatas*) as an alternative energy feedstock: processing and physicochemical characterizations, *Heliyon*, 2021, **7**, e08402.
23 H. Marsh and F. Rodriguez-Reinoso, *Activated Carbon*, Elsevier: Oxford, 2006.
24 A. A. Tadesse, Production and optimization of bioethanol from mixed banana and papaya peels using Saccharomyces cerevisiae, *Am. J. Chem. Biochem. Engg*, 2024, **8**, 45–57.
25 A. Chafidz, W. Astuti, D. Hartanto, A. S. Mutia and P. R. Sari, Preparation of activated carbon from banana peel waste for reducing air pollutant from motorcycle muffler, *EDP Sci*, 2018, **154**, 01021.
26 L. A. Al Jebur and L. H. Alwan, Development of nano-activated carbon and apply it for dyes removal from water, *Water Practice and Technology*, 2022, **17**, 297–310.
27 C. Palma, L. Lloret, A. Puen, M. Tobar and E. Contreras, Production of carbonaceous material from avocado peel

for its application as alternative adsorbent for dyes removal, Chinese J, *Chemical Eng*, 2016, **24**, 521–528.
28 A. El. Nemr, R. M. Aboughaly, S. El Sikaily, M. S. Ragab, M. S. Masoud and M. S. Ramadan, Microporous nano-activated carbon type I derived from orange peel and its application for Cr (VI) removal from aquatic environment, *Biomass Conversion and Biorefinery*, 2020, **2**, 1–9.
29 J. B. Njewa, E. Vunain and T. Biswick, Synthesis and Characterization of Activated Carbons Prepared from Agro-Wastes by Chemical Activation, *J. Chem*, 2022, **2022**, 9975444.
30 M. F. Elkady, M. M. Hussein and M. M. Salama, Synthesis and characterization of nano-activated carbon from elmaghara coal, Sinai, Egypt to be utilized for wastewater purification, *Am. J. Applied Chem*, 2015, **3**, 1–7.
31 ASTM International, D.3172, D.3173, D.3174, D.3175, West Conshohocken, PA, 2004.
32 O. O. Onawumi, A. A. Sangoremi and O. S. Bello, Preparation and characterization of activated carbon from groundnut and egg shells as viable precursors for adsorption, *J Applied Sci. and Envir. Management*, 2021, **25**, 1707–1713.
33 I. A. Tan, A. L. Ahmad and D. B. Hameed, Preparation of activated carbon from coconut husk: Optimization study on removal of 2,4,6-trichlorophenol using response surface methodology, *J. hazardous materials*, 2008, **153**, 709–717.
34 R. Ganjoo, S. Sharma, A. Kumar and M. M. Daouda, Activated carbon: Fundamentals, classification, and properties, *Book Chapter I, The Royal Soc. Chem*, 2023, 1–12.
35 G. Vijayakumar, R. Tamilarasan and M. Dharmendirakumar, Adsorption, Kinetic, Equilibrium, and Thermodynamic studies on the removal of basic dye Rhodamine-B from aqueous solution by the use of natural adsorbent perlite, *J. Mater. Environ. Sci*, 2012, **3**, 157–170.
36 O. Oginni, K. Singh, G. Oporto, B. Dawson-Andoh, L. McDonald and E. Sabolsky, Effect of one-step and two-step H_3PO_4 activation on activated carbon characteristics, Bioresource Techn, *Reports*, 2019, **8**, 100307.
37 L. M. Humphrey, G. John, M. Duncan, Local Production of high-quality cane juice and improved Jaggery products in Rang we district, Kenya, Project Report, 2011.
38 C. C. Thai, *Studies on the Clarification of Juice from Whole Sugar Cane Crop, Doctoral Dissertation*, Queensland University of Technology, 2013.
39 Z. Din and G. Rasool, Physico-chemical analysis and polarization value estimation of raw sugar from refining point of view, *American J. Plant Sci*, 2015, **6**, 1–5.
40 ICUMSA Method Book, *International Commission for Uniform Methods of Sugar Analysis*. Berlin, Germany: Bartens, 2011, 128.
41 P. W. Sangura and C. A. Serrem, Determination of Sucrose Recovery Maximization in Nzoia Sugar Factory, Kenya, *Afri. J. Edu. Sci. Technol*, 2014, **2**, 128–135.
42 L. T. Tran, M. Q. Nguyen, H. T. Hoang, H. T. Nguyen and T. H. Vu, Catalytic hydrothermal carbonization of avocado peel, *J. Chem*, 2022, 1–10.
43 H. Zheng and L. Wang, Banana peel carbon that containing functional groups applied to the selective adsorption of Au (III) from waste printed circuit boards, *Soft Nanosci. Lett*, 2013, **3**, 29–36.
44 N. A. Hamid and N. Z. Zulkifli, Papaya peels as source of hydro char via hydrothermal carbonization, *IOP Conference Series: Earth and Envir. Sci*, 2021, **765**, 01200.
45 A. Vimalkumar, J. Thilagan, K. Rajasekaran, C. Raja and M. N. Flora, Preparation of activated carbon from mixed peels of fruits with chemical activation (K_2CO_3)-application in adsorptive removal of methylene blue from aqueous solution, *Inter. J. Envir. and Waste Management*, 2018, **22**, 260–271.
46 T. Mada, R. Duraisamy and F. Guesh, Optimization and characterization of pectin extracted from banana and papaya mixed peels using response surface methodology, *Food Science & Nutrition*, 2022, **10**, 1222–1238.
47 C. Guo, L. Ding, X. Jin, H. Zhang and D. Zhang, Application of response surface methodology to optimize chromium (VI) removal from aqueous solution by cassava sludge-based activated carbon, *J. Environ. Chemi. Engg*, 2021, **9**, 104785.
48 J. Zheng, K. Wang, E. Luo, D. Wu, F. Zhu, R. Jiang, C. Su, C. Wei and G. Ouyang, Monodisperse microporous carbon nanospheres: an efficient and stable solid phase microextraction coating material, *Anal. Chim. Acta*, 2015, **884**, 44–45.
49 M. Blachnio, A. Derylo-Marczewska, B. Charmas, M. Zienkiewicz-Strzalka, V. Bogatyrov and M. Galaburda, Activated carbon from agricultural wastes for adsorption of organic pollutants, *Molecules*, 2020, **25**, 5105.
50 B. H. Hameed, A. T. M. Din and A. L. Ahmad, Adsorption of methylene blue onto bamboo- based activated carbon: Kinetics and equilibrium studies, *J. Hazard. Mate*, 2007, **141**, 819–825.
51 A. A. Ayalew and T. A. Aragaw, Utilization of treated coffee husk as low-cost bio-sorbent for adsorption of methylene blue, *Adsorption Sci. and Technology*, 2020, **38**, 205–222.
52 K. Qureshi, I. Bhatti, R. Kazi and A. K. Ansari, Physical and chemical analysis of activated carbon prepared from sugarcane bagasse and use for sugar decolorization, *Inter. J. Chemi. Biomole. Engg*, 2008, **1**, 145–149.
53 N. Nachat, P. Tobarameekul and P. Worathanakul, Activated carbon from bagasse for syrup decolorization as an alternative for waste management and the assessment of carbon footprint, Envir, *Nat. Resour. J*, 2014, **12**, 66–73.
54 M. Danish, R. Hashim, M. M. Ibrahim and O. Sulaiman, Optimized preparation for large surface area activated carbon from date (Phoenix dactylifera L.) stone biomass, *Biomass and bioenergy*, 2014, **61**, 167–178.
55 O. Ioannidou and A. Zabaniotou, Agricultural residues as precursors for activated carbon production – A review, *Renewable and Sustainable Energy Reviews*, 2007, **11**, 1966–2005.
56 K. Y. Foo and B. H. Hameed, Preparation and characterization of activated carbon from melon (*Citrullus*

vulgaris) seed hull by microwave induced NaOH activation, *Desalination Water Treat*, 2012, **47**, 130–138.
57 M. Ahmedna, W. E. Marshall and R. M. Rao, Surface properties of granular activated carbons from agricultural by-products and their effects on raw sugar decolorization, *Bioresource technology*, 2000, **71**, 103–112.
58 H. Aljohani, Y. Ahmed, O. El-Shafey, S. El-Shafey, R. Fouad and K. Shoueir, Decolorization of turbid sugar juice from sugar factory using waste powdered carbon, *Appl. Water Sci.*, 2018, **8**, 48.
59 X. Y. Cui, F. Jia, Y. X. Chen and J. Gan, Influence of single-walled carbon nanotubes on microbial availability of phenanthrene in sediment, *Ecotoxicology*, 2011, **20**, 1277–1285.
60 S. D. Gisi, G. Lofrano, M. Grassi and M. Notarnicola, Characteristic and adsorption capacities of low-cost sorbents for wastewater treatment: a review, *Sust. Mate. Technols*, 2016, **9**, 10–40.
61 V. Viena, M. Nizar and S. Wardani, Preparation of activated carbons from banana (Musa acuminate L.) peels for carbon monoxide adsorption, *Proceedings of MICoMS*, 2017, **1**, 381–386.
62 A. Ş. Yargıç, R. Y. Şahin, N. Özbay and E. Önal, Assessment of toxic copper (II) biosorption from aqueous solution by chemically-treated tomato waste, *J. Cleaner Prod*, 2015, **88**, 152–159.
63 S. Abbaszadeh, S. R. Alwi, C. Webb, N. Ghasemi and I. I. Muhamad, Treatment of lead-contaminated water using activated carbon adsorbent from locally available papaya peel biowaste, J, *Cleaner Production*, 2016, **118**, 210–222.
64 J. K. Fatombi, S. A. Osseni, E. A. Idohou, I. Agani, D. Neumeyer, M. Verelst, R. Mauricot and T. Aminou, Characterization and application of alkali-soluble polysaccharide of Carica papaya seeds for removal of indigo carmine and Congo red dyes from single and binary solutions, *J. Envir. Chemical Eng*, 2019, **7**, 103343.
65 S. Kamsonlian, C. Balomajumder and S. A. Chand, A potential of biosorbent derived from banana peel for removal of As (III) from contaminated water, *Inter. J. Chemical Sci. and Applications*, 2012, **3**, 269–275.
66 W. Jaihan, V. Mohdee, S. Sanongraj, U. Pancharoen and K. Nootong, Biosorption of lead (II) from aqueous solution using Cellulose-based Bio-adsorbents prepared from unripe papaya (Carica papaya) peel waste: Removal Efficiency, Thermodynamics, kinetics and isotherm analysis, *Arabian J. Chem*, 2022, **15**, 103883.
67 J. Maharjan and V. K. Jha, *Activated Carbon Obtained from Banana Peels for the Removal of as (III) from Water*, Scientific World, 15, 2022, 145–157.
68 V. Tucureanu, A. Matei and A. M. Avram, FTIR spectroscopy for carbon family study, *Critical reviews in analytical chemistry*, 2016, **46**, 502–520.
69 Z. Xie, X. Z. Gang, G. W. G. Wei, Ji. Fang, J. F. Ying, S. Z. Rong, S. Z, Z. Yan and Z. Y. Ling, Production of biologically activated carbon from orange peel and landfill leachate, and subsequent treatment technology, *J. Chem.*, 2014, **4**, 1–9.
70 C. Bouchelta, M. S. Medjram, O. Bertrand and J. P. Bellat, Preparation and characterization of activated carbon from date stones by physical activation with steam, *J. Analy. and Applied Pyrolysis*, 2008, **82**, 70–77.
71 W. W. Ngah and M. M. Hanafiah, Removal of heavy metal ions from wastewater by chemically modified plant wastes as adsorbents: a review, *Bioresour. Technol*, 2008, **99**, 3935–3948.
72 B. D. Cullity, and S. R. Stock, *Elements of X-Ray Diffraction*, Prentice Hall, 2001.
73 S. Rigollet, T. Beguerie, E. Weiss-Hortala, G. Flamant and A. Nzihou, Synthesis of graphitic biocarbons from lignin fostered by concentrated solar energy, *Scientific Reports*, 2025, **15**, 6418.
74 R. Ubago-Pérez, F. Carrasco-Marín, D. Fairén-Jiménez and C. Moreno-Castilla, Granular and monolithic activated carbons from KOH-activation of olive stones, *Micropor. Mesopor. Mate*, 2006, **92**, 64–70.
75 L. K. Shrestha, L. Adhikari, R. G. Shrestha, M. P. Adhikari, R. Adhikari, J. P. Hill, R. R. Pradhananga and K. Ariga, Nanoporous carbon materials with enhanced supercapacitance performance and non-aromatic chemical sensing with C1/C2 alcohol discrimination, *Sci. and Techno. Adva. MaTerialS*, 2016, **17**, 483–492.
76 M. Abbas, Experimental investigation of activated carbon prepared from apricot stone material (ASM) adsorbent for the removal of malachite green (MG) from aqueous solution, *Ads. Sci. & Techn.*, 2020, **1**, 38.
77 C. Namasivayam and D. Kavitha, Removal of Congo Red from water by adsorption onto activated carbon prepared from coir pith, an agricultural solid waste, *Dyes and Pigments*, 2002, **54**, 47–58.
78 C. Agarwal and A. K. Pandey, Remediation and recycling of inorganic acids and their green alternatives for sustainable industrial chemical processes, *Envrion, Sci. Adv*, 2023, **2**, 1306–1339.
79 P. I. Bekker and H. N. Stolz, Enhancement of sugar production part 1: Production of white sugar in the raw house, *In Procs Afar Sug Technol Ass*, 2001, **75**, 341–345.
80 K. Ravikumar, K. Pakshirajan, T. Swaminathan and K. J. Balu, Optimization of batch process parameters using response surface methodology for dye removal by a novel adsorbent, *Chemical Engineering J*, 2005, **105**, 131–138.
81 Z. Y. Zhong, Q. Yang, M. X. Li, K. Luo, Y. Liu and G. M. Zeng, Preparation of peanut hull-based activated carbon by microwave-induced phosphoric acid activation and its application in Remazol Brilliant Blue R adsorption, *J. Indu. Crops Prod*, 2012, **37**, 178–185.
82 M. T. Uddin, M. A. Islam, S. Mahmud and M. Rukanuzzaman, Adsorptive removal of methylene blue by tea waste, *J. Haz. Mate*, 2009, **164**, 53–60.
83 G. Asfaw, *Optimization of Pre-liming and Sulphation pH of Cane Juice on Clarification*, Doctoral dissertation, Addis Ababa University, 2015.

84 M. F. Majid, H. F. Zaid, C. F. Kait, K. Jumbri, L. C. Yuan and S. Rajasuriyan, Futuristic advance and perspective of deep eutectic solvents for extractive desulfurization of fuel oil: A review, *J. Molecular Liquids*, 2020, **306**, 112870.

85 M. Kosmulski, The pH dependent surface charging and points of zero charge X. Update, *Adv. in Coll. Interface Sci*, 2023, **319**, 102973.

86 El. H. Benaddi and M. R. Laamari, Facile synthesis of low-cost porous activated carbon and the adsorption properties: Characterization, optimization, kinetic models, and thermodynamic study, *The J. Chemi. Thermo.*, 2026, **214**, 107625.

87 K. Panpae, W. Jaturonrusmee, W. Mingvanish, C. Nuntiwattanawong, S. Chunwiset, K. Santudrob and S. Triphanpitak, Minimization of sucrose losses in sugar industry by pH and temperature optimization, *Malaysian J. Anal. Sci*, 2008, **12**, 513–519.

88 H. Kassa, *Handbook of Laboratory Methods and Chemical Control for Ethiopian Sugar Factories*, Ethiopian Sugar Development Agency Research Directorate, Wonji, Ethiopia, 2010.

89 H. C. De. Whalley, *ICUMSA Methods of Sugar Analysis: Official and Tentative Methods Recommended by the International Commission for Uniform Methods of Sugar Analysis (ICUMSA)*, Elsevier, 2013.

90 G. A. Abdel-Razig, I. A. Ahmed, E. E. Babiker and A. E. Yagoub, Effect of the addition of separan at different concentrations as a flocculant on the quality of sugar cane juice, *Inter. J. Nutrition and Food Eng*, 2010, **4**, 138–141.

91 H. C. C. Bourzutschky, Color formation and removal-options for the sugar and sugar refining industries: a review (part 1), *Sugar Industry*, 2005, **130**, 470–475.

92 W. Doherty and D. Rackemann, Some aspects of calcium phosphate chemistry in sugarcane clarification, *Inter. Sugar J*, 2009, **111**, 448–454.

93 O. P. Chauhan, D. Singh, S. M. Tyagi and D. K. Balyan, Studies on preservation of sugarcane juice, *Inter. J. food prop.*, 2002, **5**, 217–229.

94 K. Begum, S. Arefin, S. Islam and J. Islam, Preservation of sugarcane juice using herbal clarificant, *Int. J. Nutr. Food Sci*, 2015, **4**, 530–534.

95 ICUMSA Method Book, *International Commission for Uniform Methods of Sugar Analysis*. Berlin, Germany: Bartens,128, 2011.

96 D. Oliveira, M. M. M. Esquiaveto and J. F. S. Júnior, Sugar specification parameters and their impact on the food industry, *Food Sci. Technol*, 2007, **27**, 99–102.

97 C. C. D. Thai, H. Bakir and W. O. Doherty, Insights to the clarification of sugar cane juice expressed from sugar cane stalk and trash, *J. of Agric. Food Chem*, 2012, **60**, 2916–2923.

98 N. Ramadan, S. I. Samy El-Saylad, S. M. I. Darwish, E. A. Ramadan and M. A. Ahmed, Physicochemical properties and polarization value in raw and refined sugar, Egypt, *Sugar J.*, 2022, **19**, 1982–1990.

99 L. Rozsa, J. Rozsa and S. Kilpinen, Crystal growth and crystallization control tactics in industrial sugar crystallizers Part 1, Crystal growth, *Inter. Sugar J*, 2016, **118**, 746–755.

100 G. H. Costa, I. D. Masson, L. A. Freita, J. P. Roviero and M. J. Mutton, Use of Moringa oleífera Lamarck leaf extract as sugarcane juice clarifier: effects on clarified juice and sugar, *Food Science and Technology*, 2014, **34**, 204–209.

101 M. Saska, B. S. Zossi and H. L. Liu, Removal of color in sugar cane juice clarification by defecation, sulfitation and carbonation, *Inter. Sugar J*, 2010, **112**, 258–260.

102 B. Andrzejewski, G. Eggleston, S. Lingle and R. Powell, Development of a sweet sorghum juice clarification method in the manufacture of industrial feedstocks for value-added fermentation products, *Indus. Crops Prod*, 2013, **44**, 77–87.

103 A. F. Zailer, R. N. T. Vania, B. O. Eduardo, D. S. Jane and J. Selia, Telis-Romero, Rheology and fluid dynamics properties of sugarcane juice, *Biochem. Engg. J*, 2011, **53**, 260–265.

104 Brazil National Sanitary Surveillance: *Resolution Board of National Sanitary Surveillance*, 2003, 175.

105 P. W. Rein, L. S. M. Bento and R. Cortes, The direct production of white sugar in a cane sugar mill. Inte, *Sugar J*, 2007, **109**, 286–299.

106 P. Umesh Kumar, B. Birendra Kumar and N. Padmalochan, Green synthesis and characterization of gold nanoparticles using onion (*Allium cepa*) extract, *World J. Nano Sci. Engg*, 2011, **1**, 93–98.

107 R. C. Bansal and M. A. Goyal, *Activated Carbon Adsorption*, CRC Press, 2005.